ACS Chemical Neuroscience

pubs.acs.org/chemneuro Research Article

Neuroprotective Effects of Trehalose and Sodium Butyrate on Preformed Fibrillar Form of α-Synuclein-Induced Rat Model of Parkinson's Disease

Violina Kakoty, Sarathlal K C, Sunil Kumar Dubey, Chih-Hao Yang, and Rajeev Taliyan*

Cite This: ACS Chem. Neurosci. 2021, 12, 2643−2660 Read Online

ACCESS | Metrics & More | Article Recommendations | Supporting Information

ABSTRACT: Therapeutic options for Parkinson's disease (PD) are limited to a symptomatic approach, making it a global threat. Targeting aggregated alpha-synuclein (α-syn) clearance is a gold standard for ameliorating PD pathology, bringing autophagy into the limelight. Expression of autophagy related genes are under the regulation by histone modifications, however, its relevance in PD is yet to be established. Here, preformed fibrillar form (PFF) of α-syn was used to induce PD in wistar rats, which were thereafter subjected to treatment with trehalose (tre, 4g/kg, orally), a potent autophagy inducer and sodium butyrate (SB, 300 mg/kg, orally), a pan histone deacetylase inhibitor alone as well as in combination. The combination treatment significantly reduced motor deficits as evidenced after rotarod, narrow beam walk, and open field tests. Novel object location and recognition tests were performed to govern cognitive abnormality associated with advanced stage PD, which was overcome by the combination treatment. Additionally, with the combination, the level of pro-inflammatory cytokines were significantly reduced, along with elevated levels of dopamine and histone H3 acetylation. Further, mRNA analysis revealed that levels of certain autophagy related genes and proteins implicated in PD pathogenesis significantly improved after administration of both tre and SB. Immunofluorescence and H&E staining in the substantia nigra region mirrored a potential improvement after treatment with both tre and SB. Therefore, outcomes of the present study were adequate to prove that combinatorial efficacy with tre and SB may prove to be a formidable insight into ameliorating PD exacerbated by PFF α-syn as compared to its individual efficacy.

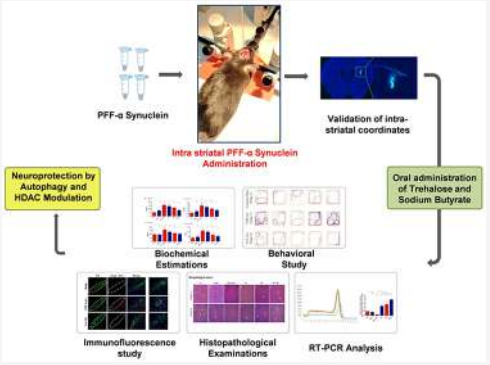

KEYWORDS: *Parkinson's disease, preformed fibrillar form of alpha-synuclein, autophagy, epigenetics, trehalose, sodium butyrate*

Downloaded via BITS PILANI PILANI CAMPUS on August 26, 2021 at 05:42:23 (UTC).
See https://pubs.acs.org/sharingguidelines for options on how to legitimately share published articles.

INTRODUCTION

Next to Alzheimer's disease (AD), Parkinson's disease (PD) is found to affect the worldwide population at a rate of 0.3% and 3% of those in the age group of 80 years.[1] Over 200 years ago, James Parkinson's essay on the Shaking Palsy became a driving force for digging deep into the underlying etiology of PD;[2] still the only available therapeutic approach is based on symptomatic management. Slowness of movement, postural instability, rigidity, and tremor are some of the major motor features associated with PD.

Motor symptoms mainly occur due to dopamine (DA) loss in the substantia nigra pars compacta (SN) and its downstream impairment of basal ganglia activity.[3] Up to 80% of PD patients experience PD dementia (PDD) as the disease progresses,[4] and cognitive abnormality is also known to occur before the motor symptoms onset or can build up as the disease progresses.[5] Neuropathologically, presence of lewy bodies (LBs) characterizes both PD and PDD as devised by Friedrich Lewy in 1912,[6] and this led to the identification of alpha-synuclein (α-syn) as the primary component of LBs.[7]

α-Syn is a cytosolic protein and normally localized in the presynaptic terminals.[8] Once the neuron is affected, α-syn forms LBs in its soma.[9] α-Syn inclusions initiate its formation over greater periods of time which might result in the LBs affecting only a subset of neurones.[3] However, neurones can also be affected by α-syn due to uptake of these inclusions by synaptically connected neurons as evidenced by recent data from humans and model systems, leading to a pathological spread within the brain that correlates with disease progression. Progressive loss of motor coordination is the major symptom of PD, attributable to dysregulation of basal ganglia activity that is largely due to the degeneration of DA neurons in the SN.[9] However, at advanced stages of the

Received: March 13, 2021
Accepted: June 17, 2021
Published: July 1, 2021

© 2021 American Chemical Society

https://doi.org/10.1021/acschemneuro.1c00144
ACS Chem. Neurosci. 2021, 12, 2643−2660

disease, it has been found that α-synucleinopathy might spread to other brain regions including limbic areas, the neocortical region, and the brainstem.[10]

Evidence suggests that the preformed fibrillar form (PFF) of α-syn (hereby referred to as PFF α-syn) is the most toxic oligomeric form of α-syn and has been accepted as a well-established model for PD induction both *in vivo* and *in vitro*.[11] Normally, α-syn is degraded by the chaperone-mediated form (CMA) of autophagy.[12] Autophagy, a self-degradative mechanism, is responsible for disposing of damaged proteins, maintaining the body decorum orchestrated by CMA and micro and macroautophagy. Aggregated/mutant forms of α-syn, for instance, its PFF form, inhibit CMA, evoking an accumulation of damaged proteins and degenerating neurones with time. However, a study suggested that cell survival can be augmented through the vesicular protein sorting 34-beclin-1 complex, a secondary signaling pathway for autophagy initiation where beclin-1 overexpression causes reduced α-syn accumulation, decreases cell death, and enhances lysosomal degradation,[13] delineating the fact that enhancement in autophagy clears out aggregated proteins and its tailored manipulation can help reduce PD pathology.

Trending research has confirmed the role of trehalose (tre) as an inducer of autophagy in various neurodegenerative models, mainly attributed to its neuroprotective potential though microbiota-gut-brain signaling.[14] This hypothesis was further strengthened when it was established that autophagy induction in the mouse brain took place only after an oral intake of tre, suggesting that the gastrointestinal (GI) system[15] plays a crucial role in the neuroprotective mechanism by tre. Moreover, Martano et al. reported that the mouse hippocampus and cortex evidenced the presence of tre. Endogenous tre was present in astrocytes and neurons with its hydrolyzing enzyme, trehalase, present in neurons. Release of tre into the extracellular space[16] was facilitated by the astrocytes.

Treatment of tre to prion infected cells elevated microtubule-associated protein 1A/1B-light chain 3-phosphatidylethanolamine conjugate (LC3-II) levels, increasing the basal levels of autophagy.[17] In the same study, *de novo* production of PrPSc aggregates was reduced along with its subcellular localizations alteration. An autophagic substrate, namely, p62/SQSTM1, was decreased by oral delivery of tre to Parkin−/−/TauVLW mice. Tre also prevented cell death induction due to polyubiquitinated proteins activated by a proteasome inhibitor, epoxomicin.[18] Tre altered epoxomicin-induced autophagic inhibition, as evidenced by normal levels of LC3-II and p62/SQSTM1. In another study, an oral delivery of 1% tre (approximately 1.9−2.3 g/kg) for 28 days could not reverse the 1-methyl-4-phenyl-1,2,3,6-tetrahydropyridine (MPTP) induced behavioral changes in C57Bl/6 mice; however, the treatment could decrease the striatal DA, homovanillic acid (HVA), and 3,4-dihydroxyphenylacetic acid (DOPAC).[19] Sarkar et al. demonstrated that treatment with 2% of tre twice weekly for 5 weeks on MPTP induced PD on C57Bl/6 mice and decreased the MPTP induced loss in DA transporter and tyrosine hydroxylase (TH) in the caudate/putamen (CPU) and SnPC along with improved motor abnormalities.[20] In another study, rat's injected with human A53T α-syn expressed virus vector underwent treatment with 0.5, 2 and 5% of tre for 6 weeks. The 0.5% tre treatment failed to improve neurochemical and behavioral deficits. However, 2 and 5% tre treatment could improve motor abnormalities, neurodegeneration, and α-syn aggregation in the nigrostriatal system and elevated striatum LC3-II levels.[21]

Further, histone post-translational modification causes autophagy induction, as confirmed by a study conducted by Madeo, Kroemer, and co-workers, where, upon treatment with spermidine in aging yeast, the cytoprotective autophagy activation occurred due to histone acetylation inhibition, specifically, Iki3 and Sas3, rendering global histone H3 hypoacetylation, with the repression of gene expression. Additionally, autophagy induction by numerous stimuli decreases the acetylation of histone H4 lysine 16 (H4K16ac). H4K16 deacetylation invokes a decreased level in the expression of autophagy-related genes, such as, ATG9A, MAP1LC3, GABARAPL2, VMP1, ULK1, and ULK3.[22] Inhibition of the autophagic H4K16 deacetylation increases autophagic flux instead of inhibiting autophagy, proving the outcomes of several experimental reports which are consistent with genome-wide investigations. Similarly, di and trimethylation of histone H3 at lysine 4[23] and H4K20[24] control the expression of major autophagy related genes, modulating transcriptional activation and repression. Lower histone acetylation levels are observed in AD and PD models,[25] for instance, a histone deacetylase inhibitor (HDACi), and valproic acid was found to be neuroprotective against rotenone induced PD.[26] Sodium butyrate (SB), a pan HDACi, can elicit major neuroprotective potency against 6-hydroxydopamine induced PD in rats in lieu of its histone acetylation action and great blood−brain barrier permeability as reported previously from our lab.[27] However, whether the neuroprotective efficacy of HDACi such as valproic acid and SB via autophagy modulation remains largely unknown.

Hence, in the current study, PFF α-syn was used to induce PD in wistar rats. Six months after complete pathology formation, the rats were administered with an autophagy inducer, that is, tre and a pan HDACi, SB. These drugs were administered singly and in combination to investigate their resultant effects on the behavioral outcome, expression of certain autophagy related genes, neuroinflammatory markers, pyknotic neuronal count, and percentage positive cells for relevant proteins known to directly influence progression of PD pathology.

RESULTS AND DISCUSSION

Validation of Intrastriatal Coordinates. Before proceeding with the induction of PD on all the animals using PFF α-syn, first the selected intrastriatal coordinates were validated by injection of a green fluorescent protein (GFP) directly into the striatum. At 48 h post-injection, the animal was sacrificed, the brain was isolated as per standard immunofluorescence (IFC) protocol, and staining with DAPI was performed on the striatum section of the brain (Supplementary Figure 1).

Effect of tre and SB on Rotarod Test. The rotarod test has been widely accepted as a model for assessment of motor abnormality disorder. During the test, the animals injected with PFF α-syn had a decreased fall of time from the revolving rod in comparison with sham control animals. The group treated with tre alone does not have any significant difference when compared with the disease group, whereas the group treated with SB alone had a faintly improved condition (***$P \leq 0.001$), but the group treated with a combination of tre and SB had a significant rise in the fall of time (****$P \leq 0.0001$) from the revolving rod on comparison with the disease group. Moreover, in the combination group, a significant increase in

https://doi.org/10.1021/acschemneuro.1c00144
ACS Chem. Neurosci. 2021, 12, 2643−2660

the fall of time was observed when compared with tre (****$P \leq 0.0001$), but not with SB (Figure 1).

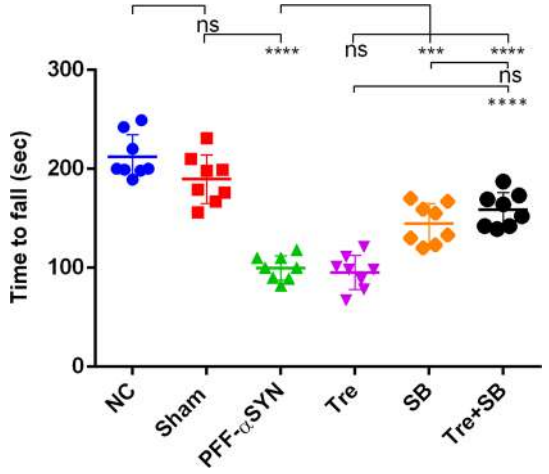

Figure 1. Effect of tre and SB on rotarod test. Values represents mean ± SD, ****$P \leq 0.0001$ (sham vs PFF α-syn); ns (PFF α-syn vs tre); ***$P \leq 0.001$ (PFF α-syn vs SB); ****$P \leq 0.0001$ (PFF α-syn vs tre +SB); ****$P \leq 0.0001$ (tre+SB vs tre); ns (tre+SB vs SB), $F(5,42) = 46.54$, $P < 0.0001$, ns: nonsignificant, NC: normal control.

Effect of tre and SB on Open Field Test. The open field test is mainly used to access any abnormality related to locomotor activity and speed of locomotion of the animals that might result in immobility. Due to its ease of use and easily distinguishable features, this test provides an unbiased conclusion of the degree of severity of PD. During the test, the total distance traveled by each animal was calculated, where it was observed that the distance traveled was reduced in the case of diseased animals (****$P \leq 0.0001$) upon comparison with the sham control group. The group treated with tre alone had a nonsignificant difference in distance traveled when compared to the disease group. However, a statistically significant result was observed in the group administered with SB alone (*$P \leq 0.05$) and the combination treated group, that is, tre and SB (****$P \leq 0.0001$). Further, in the combination group, the distance traveled was significantly increased when compared with tre (****$P \leq 0.0001$) but not with SB, suggesting that the combination group might possess an increased therapeutic potency as compared to either of the drugs alone (Figure 2).

Effect of tre and SB on NBW Test. The NBW test is widely used to rule out gait abnormalities in a PD induced animal. During the test, the analysis is done by measuring the duration of the animal to reach the platform. Here, the diseased group took a longer time to reach the home cage (****$P \leq 0.0001$) as compared to the sham control group and the treated groups. The combination group had a statistically significant decrease (****$P \leq 0.0001$) in the amount of time taken to reach the target platform, and a similar case was observed with the group treated with SB alone (****$P \leq 0.0001$) when compared with the disease group. However, the group treated with tre alone had no significant difference. Further, the combination group demonstrated a significant decrease in the duration to reach the platform when compared with tre (****$P \leq 0.0001$), but not with SB (Figure 3). Additionally, the number of foot paw slips was analyzed in this test, and the slips were decreased in the treated group with SB

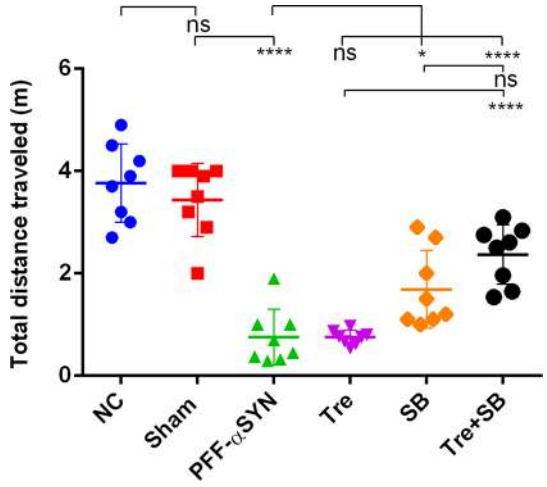

Figure 2. Effect of tre and SB on total distance traveled. Values represent mean ± SD, ****$P \leq 0.0001$, (sham vs PFF α-syn); ns (PFF α-syn vs tre); *$P \leq 0.05$ (PFF α-syn vs SB); ****$P \leq 0.0001$ (PFF α-syn vs tre+SB); ****$P \leq 0.0001$ (tre+SB vs tre); ns (tre+SB vs SB), $F(5,42) = 34.85$, $P < 0.0001$, ns: nonsignificant, NC: normal control.

alone (**$P \leq 0.01$), with a more pronounced effect observed in the combination group (****$P \leq 0.0001$) in comparison with the disease group and no significance observed for the tre group. Moreover, in the combination group compared with tre, a significant decrease in paw slip was observed (****$P \leq 0.0001$) but not with SB treatment (Figure 3).

Effect of tre and SB on NOR and NOL Test. The NOR and NOL test is a widely known model to govern any cognitive anomaly present in rodents. Studies suggest that PD is associated with cognitive disturbances either at an advanced stage of the disease or as a prewarning sign before the occurrence of its pathology. Having said this, it is extremely necessary to perform a memory recognition task to accurately speculate the progression of PD pathology and its amelioration by the treated groups. The task consisted of four stages:

- Stage 1: The animals could freely roam in an open field, and the results were found to be statistically insignificant for all the groups at this stage, as shown in Figure 4A (quantified image is given as supplementary Figure 3a).
- Stage 2: The animals were trained in the presence of two similar objects, as shown in Figure 4B, where the sham control group had an increased tendency to explore upon comparison to disease group (***$P \leq 0.001$), but all the treated groups had a statistically insignificant result (quantified image is given as supplementary Figure 3b).
- Stage 3: The animals were provided with an acquainted or familiar and an unacquainted or novel object, as shown in Figure 4C, where a significant object recognition quality for SB (**$P \leq 0.01$) and in the combination group, that is, tre and SB (****$P \leq 0.0001$), was observed upon comparison with the diseased group. Moreover, the combination group demonstrated a significant increase in time traversed when compared with tre and SB treatments alone (****$P \leq 0.0001$ for both tre+SB vs tre and tre+SB vs SB). The discrimination index demonstrates a significant increase in tre, SB, and combination groups when compared with the disease group (****$P \leq 0.0001$, for

https://doi.org/10.1021/acschemneuro.1c00144
ACS Chem. Neurosci. 2021, 12, 2643−2660

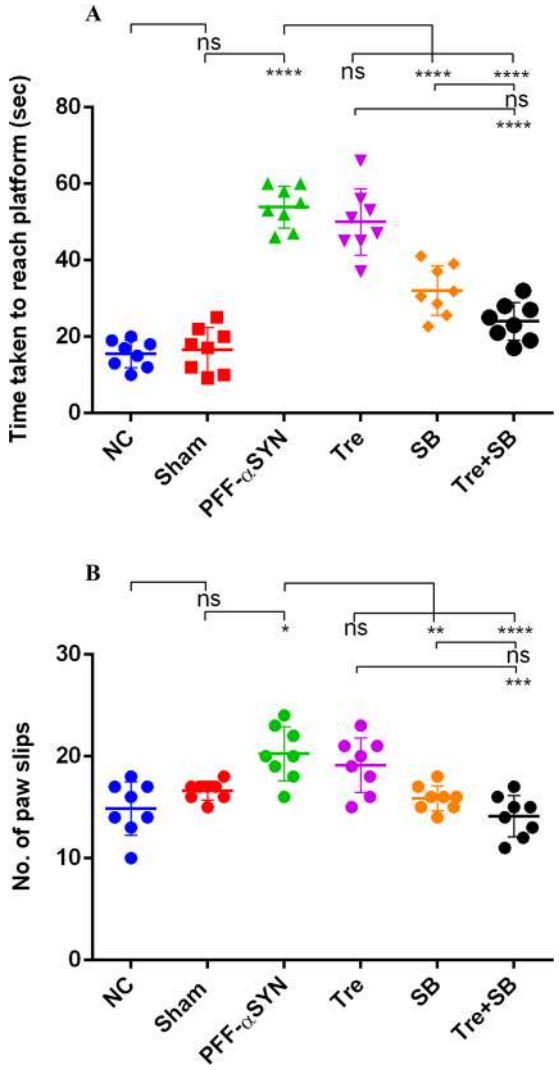

Figure 3. (A) Effect of tre and SB on time taken to reach the platform. Values represent mean ± SD, $^{****}P \leq 0.0001$, (sham vs PFF α-syn); ns (PFF α-syn vs tre), $^{****}P \leq 0.0001$ (PFF α-syn vs SB); $^{****}P \leq 0.0001$ (PFF α-syn vs tre+SB); $^{****}P \leq 0.0001$ (tre +SB vs tre); ns (tre+SB vs SB), $F(5,42) = 60.31$, $P < 0.0001$, ns: nonsignificant, NC: normal control. (B) Effect of tre and SB on number of foot paw slips. Values represent mean ± SD, $^{*}P \leq 0.05$ (sham vs PFF α-syn); ns (PFF α-syn vs tre); $^{**}P \leq 0.01$ (PFF α-syn vs SB); $^{****}P \leq 0.0001$ (PFF α-syn vs tre+SB); $^{***}P \leq 0.001$ (tre +SB vs tre); ns (tre+SB vs SB), $F(5,42) = 10.02$, $P < 0.0001$, ns: nonsignificant, NC: normal control.

all group vs PFF α-syn) (quantified image for total time traversed and discrimination index is given as supplementary Figure 3c,d respectively).

- Stage 4: The animals were presented with one familiar object but with a new location for one of the objects, as shown in Figure 4D. It was observed that the combination group had a potent effect in the location test when compared to the disease group ($^{****}P \leq 0.0001$), whereas tre and SB treated groups had little significant difference when compared with the disease group ($^{*}P \leq 0.05$ and $^{**}P \leq 0.01$ respectively). However, a significant change was observed in the combination group when compared with tre and SB ($^{***}P \leq 0.001$ and $^{**}P \leq 0.01$, respectively). The discrimination index indicates a marked significant difference in tre, SB, and combination ($^{****}P \leq 0.0001$) groups when compared with the disease group. In addition, the combination group had a significant increase in discrimination index when compared with tre ($^{*}P \leq 0.05$) (quantified image for total time traversed and discrimination index is given as supplementary Figure 3e,f respectively).

The movement of each animal was tracked and recorded using ANYMAZE software (Stoelting, USA) (Figure 4A−D). The total distance traversed by the animal and the discrimination index were calculated using the formula below and quantified using graph pad prism software:

$$\text{discrimination index} = \frac{(\text{time with novel object or location} - \text{time with familiar object or location})}{(\text{time with novel object or location} + \text{time with familiar object or location})}$$

Effect of tre and SB on TNF-α, IL-1, and IL-6 Levels. PD pathology is accompanied by extensive loss of DA neurones in the SN. Evidence strongly points toward the extreme sensitivity of DA neurones for TNF-α, IL-1, and IL-6. The levels of these inflammatory markers drastically increase in the case of the experimental PD models. In the present study, we estimated the levels of TNF-α, IL-1, and IL-6 using a commercially available ELISA kit and found that their levels increased in PD induced animals on comparison with the sham group ($^{****}P \leq 0.0001$), but the levels were found to decrease in the case of the combination treated group ($^{****}P \leq 0.0001$) when compared to the disease group. However, little significant difference was observed for the group treated with SB alone ($^{*}P \leq 0.05$, for TNF-α; $^{***}P \leq 0.001$, for IL-1 and IL-6), and no statistical significance was observed for the group treated with tre alone in the hippocampal region. Further, when the combination group was compared with treatments alone, a significant decrease was observed with tre ($^{**}P \leq 0.01$) but not with SB for TNF-α, and similarly for IL-1, tre +SB vs tre shows a significant change of $^{*}P \leq 0.05$. The level of IL-6 was found significantly diminished in the combination group when compared with treatments alone, $^{****}P \leq 0.001$ for tre+SB vs tre and $^{**}P \leq 0.01$ for tre+SB vs SB, which suggests a better suppression of neuroinflammation in the combination group when compared with single administration (Figure 5A−C). To better arrive at a conclusion, we also performed an estimation of these cytokines for the nigra region, where we observed a similar decreasing trend in the neuroinflamatory markers; same as that in the hippocampal region on treatment with tre, SB alone, and in combination (Figure 6A−C).

Effect of tre and SB on Levels of CRP. CRP is an acute-phase protein and considered an intensive biomarker of systemic inflammation. In neurodegenerative disorders like PD and AD, an increase in the levels of CRP is indicative of the severity of neurodegenerative pathology. Hence in the current study, we analyzed the expression of CRP and found that PFF α-syn markedly elevated CRP levels ($^{****}P \leq 0.0001$) on comparison with the sham group, indicating the progression of inflammatory process in that group. However, the combination group ($^{****}P \leq 0.0001$) and the group treated with SB alone ($^{***}P \leq 0.001$) markedly reduced the CRP levels compared to the disease group. For the tre treatment alone, a decreased level of CRP was observed, but it was not significant when compared with disease group. Further, upon comparing the combination group with tre and SB treatments alone, a

https://doi.org/10.1021/acschemneuro.1c00144
ACS Chem. Neurosci. 2021, 12, 2643−2660

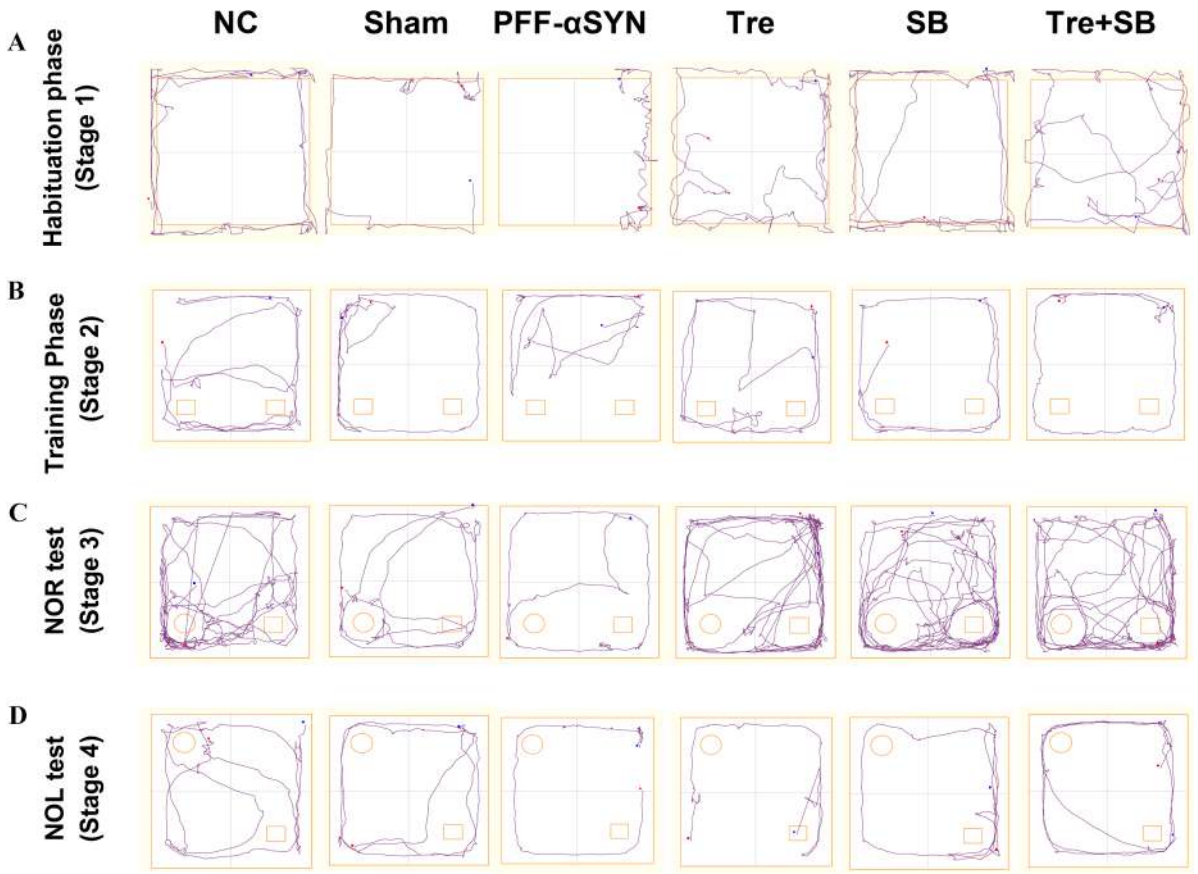

Figure 4. Track plots of animals traversed during (A) habituation phase, (B) training phase, (C) NOR, and (D) NOL tests.

significant decrease in CRP was observed with tre (****$P \leq$ 0.0001) and SB (**$P \leq$ 0.01) (Figure 7).

Effect of tre and SB on Levels of BDNF. The main function of BDNF lies in its ability to influence neuronal development, neurogenesis, synaptogenesis, synaptic plasticity, and cell differentiation. Normally, BDNF is known to regenerate DA neurones, increasing its survival and ultimately improving the motor performance which is reversed during PD.[28] In this study, we conducted an ELISA assay for BDNF to assess whether BDNF levels can be restored by treatment with tre and SB. We observed that PFF α-syn induced animals had a decreased expression of BDNF (****$P \leq$ 0.001) on comparison with the sham control, which was efficiently restored in the groups treated with the SB alone (***$P \leq$ 0.001) and in combination of tre and SB (****$P \leq$ 0.0001). No statistical difference was observed for the group treated with tre alone. Further, the combination group demonstrated a significant increase in expression level in contrast to that of tre (****$P \leq$ 0.0001) and SB (***$P \leq$ 0.001) alone treatment (Figure 8).

Effect of tre and SB on Levels of DA. The predominant pathology arising during PD is loss of DA neurones exclusively in the SN region of the brain, degenerating the region over time and affecting movement control in an individual. Here, we went on to further check the levels of DA before and after treatment with tre and SB and found that DA levels were considerably reduced in the PFF α-syn group (****$P \leq$ 0.0001) in contrast to that of the sham group and significantly restored on administration with SB alone (***$P \leq$ 0.001) and in combination with tre and SB groups (****$P \leq$ 0.0001). The animal group administered with tre alone was found to be statistically nonsignificant. However, when the combination group was compared with treatments alone, a marked increase in DA level was observed, as ****$P \leq$ 0.0001 for tre+SB vs tre and **$P \leq$ 0.01 tre+SB vs SB (Figure 9A).

Results from the DA estimation for the striatum region revealed similar results as that of the SN region when compared to the disease group with a significant increase observed for the tre group (*$P \leq$ 0.05). The combination group when compared with treatments alone also demonstrated a significant increase in DA, as ***$P \leq$ 0.001 for tre +SB vs tre and *$P \leq$ 0.05 tre+SB vs SB (Figure 9B).

Effect of tre and SB on Levels of Global Histone H3 Acetylation. PD pathogenesis is associated with several epigenetic modifications that are also known to regulate expression of autophagy related genes. The predominant component of LBs, that is, α-syn, is known to decrease histone H3 acetylation levels in cultured cells, leading to cell death.[29] Hence, we explored the global histone H3 acetylation level to assess the harmful effect of PFF α-syn and effective reversal by tre and SB. Intriguingly, we observed that reduced H3 acetylation levels were evidenced in the group of PFF α-syn when compared to the sham control group (****$P \leq$ 0.0001), which was significantly upregulated on administration with tre, SB alone (*$P \leq$ 0.05 and **$P \leq$ 0.01 respectively), and tre and SB in combination (****$P \leq$ 0.0001). Moreover, in the combination group, histone acetylation was significantly increased in comparison with tre and SB treatments alone, as ***$P \leq$ 0.001 for tre+SB vs tre and **$P \leq$ 0.01 for tre+SB vs SB (Figure 10).

Effect of tre and SB on Various mRNA Expressions. The initiating step in autophagosome assembly from

https://doi.org/10.1021/acschemneuro.1c00144
ACS Chem. Neurosci. 2021, 12, 2643−2660

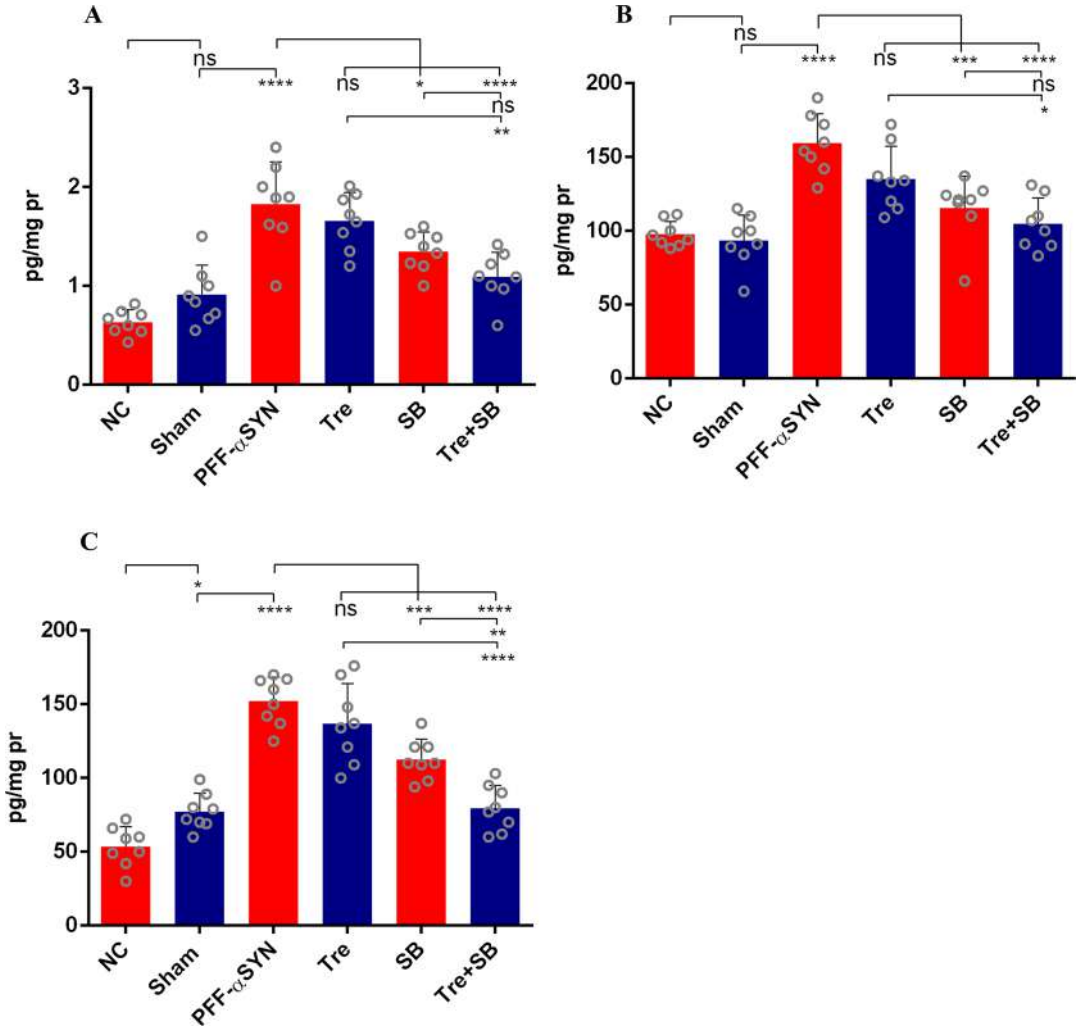

Figure 5. (A) Effect of tre and SB on TNF-α levels in hippocampal region. Values represent mean ± SD, ****$P \leq 0.0001$ (sham vs PFF α-syn); ns (PFF α-syn vs tre); *$P \leq 0.05$ (PFF α-syn vs SB); ****$P \leq 0.0001$ (PFF α-syn vs tre+SB); **$P \leq 0.01$ (tre+SB vs tre); ns (tre+SB vs SB), $F(5,42) = 20.93$, $P < 0.0001$. (B) Effect of tre and SB on IL-1 levels. Values represent mean ± SD, ****$P \leq 0.0001$ (sham vs PFF α-syn); ns (PFF α-syn vs tre); ***$P \leq 0.001$ (PFF α-syn vs SB); ****$P \leq 0.001$ (PFF α-syn vs tre+SB); *$P \leq 0.05$ (tre+SB vs tre); ns (tre+SB vs SB), $F(5,42) = 15.18$, $P < 0.0001$. (C) Effect of tre and SB on IL-6 levels. Values represent mean ± SD, ****$P \leq 0.0001$, (sham vs PFF α-syn); ns (PFF α-syn vs tre); ***$P \leq 0.001$ (PFF α-syn vs SB);****$P \leq 0.001$ (PFF α-syn vs tre+SB); ****$P \leq 0.0001$ (tre+SB vs tre); **$P \leq 0.01$ (tre+SB vs SB), $F(5,42) = 39.65$, $P < 0.0001$, ns: nonsignificant, NC: normal control.

preautophagic structures is orchestrated by a 60 kDa protein, beclin-1. In PD, the beclin-1 level is found to reduce with increasing α-syn accumulation, suggesting alterations in the process of autophagy.[30] Therefore, examining the mRNA expression of beclin-1 would provide conclusive evidence about PD progression and its effective amelioration by the respective treatments. It was observed that the PFF α-syn group had a decreased expression of beclin-1 when compared with the sham group (****$P \leq 0.0001$). However, the expression level of beclin-1 was found to significantly increase with tre (****$P \leq 0.0001$) and SB (****$P \leq 0.0001$) alone and tre and SB in combination (****$P \leq 0.0001$) treatments when compared with the disease group. Further, the combination group in comparison with treatments alone also demonstrated a significant increase in the expression of beclin-1 (****$P \leq 0.0001$) for both tre+SB vs tre and tre+SB vs SB (Figure 11A).

LC3-II is produced upon conjugation of LC3-II to phosphatidylethanolamine (PE) on the surface of nascent autophagosomes. In PD, a deficiency of LC3-II to form autophagosomes might impair the overall machinery of autophagy in clearing out aggregate-prone proteins.[31] Hence, we analyzed the mRNA levels of LC3-II and observed that the group with PFF α-syn had an impaired level of LC3-II when compared to the sham group (****$P \leq 0.0001$), and treatment with tre and SB alone improved the levels of LC3-II (****$P \leq 0.0001$). Similarly, the combined administration of tre and SB also significantly increased LC3-II expression level (****$P \leq 0.0001$) when compared with the disease group. In addition, the combination group when compared with treatments alone also shows a significant rise in the LC3-II expression level, as ****$P \leq 0.0001$ for both tre+SB vs tre and tre+SB vs SB (Figure 11B).

Lysosomal stability and autophagy require LAMP-2. In neurodegenerative conditions like PD, reduced levels of LAMP-2 are evidenced in LBs of the SN and also in the amygdala. Therefore, we examined the expression level of LAMP-2 to better arrive at a conclusion of the severity of PD pathogenesis and its effective reversal by treatments. It was observed that the PFF α-syn administration decreased the

https://doi.org/10.1021/acschemneuro.1c00144
ACS Chem. Neurosci. 2021, 12, 2643−2660

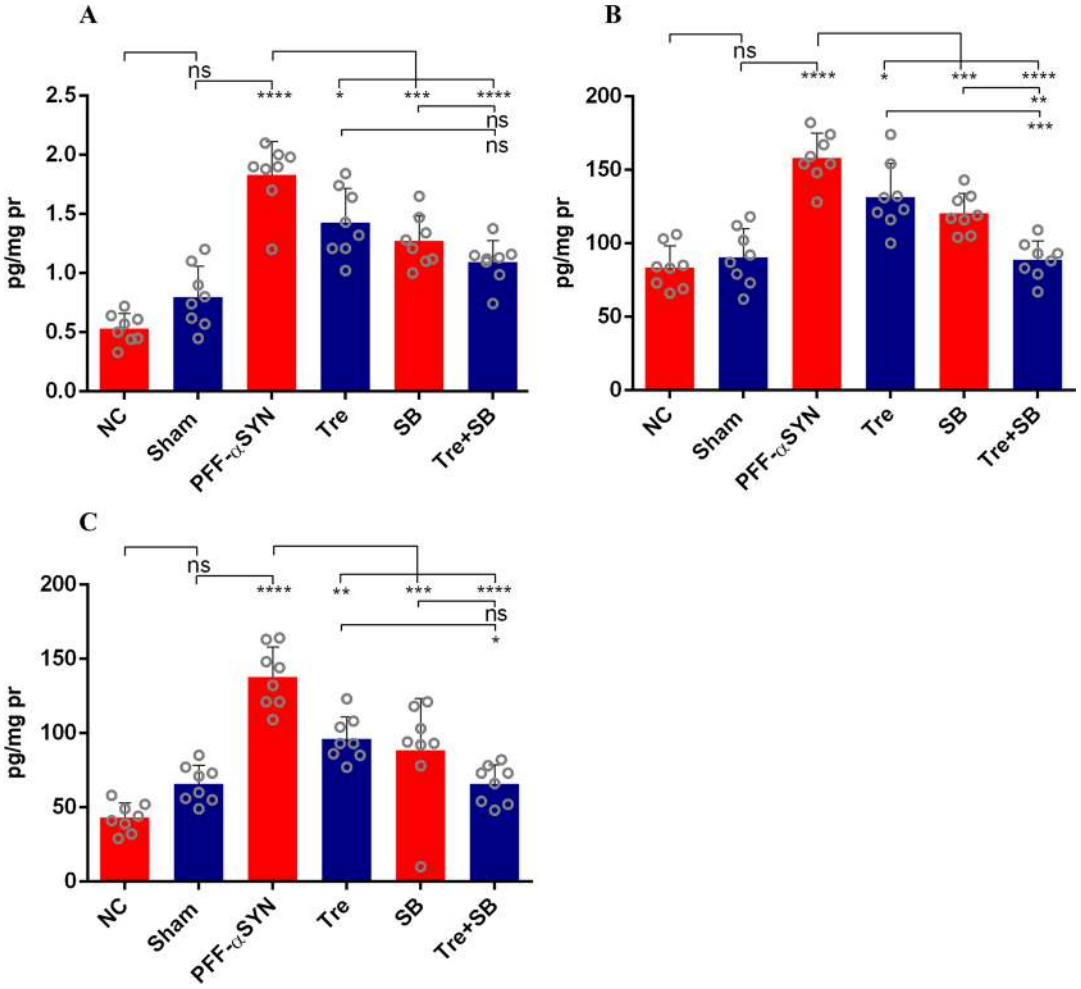

Figure 6. (A) Effect of tre and SB on TNF-α levels in nigra region. Values represent mean ± SD, ****$P \leq 0.0001$ (sham vs PFF α-syn); *$P \leq 0.05$ (PFF α-syn vs tre); ***$P \leq 0.001$ (PFF α-syn vs SB); ****$P \leq 0.0001$ (PFF α-syn vs tre+SB); ns (tre+SB vs tre); ns (tre+SB vs SB), $F(5,42) = 31.69$, $P < 0.0001$. (B) Effect of tre and SB on IL-1 levels. Values represent mean ± SD, ****$P \leq 0.0001$ (sham vs PFF α-syn); *$P \leq 0.05$ (PFF α-syn vs tre); ***$P \leq 0.001$ (PFF α-syn vs SB); ****$P \leq 0.0001$ (PFF α-syn vs tre+SB); ***$P \leq 0.001$ (tre+SB vs tre); **$P \leq 0.01$ (tre+SB vs SB), $F(5,42) = 24.12$, $P < 0.0001$. (C) Effect of tre and SB on IL-6 levels. Values represent mean ± SD, ****$P \leq 0.0001$ (sham vs PFF α-syn); **$P \leq 0.01$ (PFF α-syn vs tre); ***$P \leq 0.001$ (PFF α-syn vs SB); ****$P \leq 0.0001$ (PFF α-syn vs tre+SB); *$P \leq 0.05$ (tre+SB vs tre); ns (tre+SB vs SB), $F(5,42) = 22.89$, $P < 0.0001$, ns: nonsignificant, NC: normal control.

LAMP-2 expression on comparison with the sham group (****$P \leq 0.0001$), while an improvement was observed in the SB alone treated group (***$P \leq 0.001$). However, a marked increase in the mRNA expression level of LAMP-2 was found on administration with tre and SB in combination (****$P \leq 0.0001$). No significant change was observed for the group treated with tre alone. Moreover, the combination group revealed a significant increase in LAMP-2 expression when compared with tre and SB alone, as ****$P \leq 0.0001$ for both tre+SB vs tre and tre+SB vs SB (Figure 11C).

TH is an enzyme mainly catalyzing the rate-limiting step for the synthesis of DA via formation of L-dihydroxyphenylalanine (L-DOPA). Moreover, the early depletion of TH activity and subsequent reduction in TH protein accounts for the deficiency in DA and phenotypic expression of PD.[32] However, upon analyzing TH mRNA expression in the current study, a considerable decrease was observed in the PFF α-syn group when compared to the sham group (****$P \leq 0.0001$), followed by an enhancement in TH mRNA expression after treatment with tre (not significant) and SB (****$P \leq 0.0001$) alone and with a combination of tre and SB (****$P \leq 0.0001$). In addition, a significant increase in TH mRNA expression was found in the combination group when compared to the tre and SB treatments alone, as ****$P \leq 0.0001$ for both tre+SB vs tre and tre+SB vs SB (Figure 11D).

DAT is primarily known to regulate synaptic DA concentration in the striatum, affecting locomotor activity. During PD, loss of DAT severely hampers DA clearance, resulting in motor abnormalities. Upon analyzing the mRNA expression levels of DAT, we observed that the PD induced group had a considerable decrease in its expression on comparison with the control group (****$P \leq 0.0001$). However, the treatment with tre and SB alone and their combination increased the levels of DAT mRNA expression (*$P \leq 0.05$, ****$P \leq 0.0001$, ****$P \leq 0.0001$ respectively). Further, the combination group compared with tre and SB alone significantly elevated DAT expression, as ****$P \leq 0.0001$ for both tre+SB vs tre and tre+SB vs SB (Figure 11E).

The presynaptic protein, α-syn, shares a close relation with the pathogenesis of PD. From a plethora of available hypotheses linking α-syn and PD, the most common is the fact that the soluble fibrillar form of α-syn, namely its PFF

https://doi.org/10.1021/acschemneuro.1c00144
ACS Chem. Neurosci. 2021, 12, 2643−2660

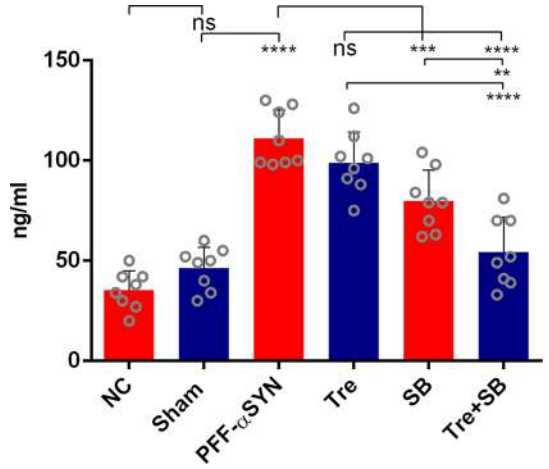

Figure 7. Effect of tre and SB on CRP levels. Values represent mean ± SD, ****$P \leq 0.0001$ (sham vs PFF α-syn); ns (PFF α-syn vs tre); ***$P \leq 0.001$ (PFF α-syn vs SB); ****$P \leq 0.0001$ (PFF α-syn vs tre +SB); ****$P \leq 0.0001$ (tre+SB vs tre); **$P \leq 0.01$ (tre+SB vs SB), $F(5,42) = 37.66$, $P < 0.0001$, ns: nonsignificant, NC: normal control.

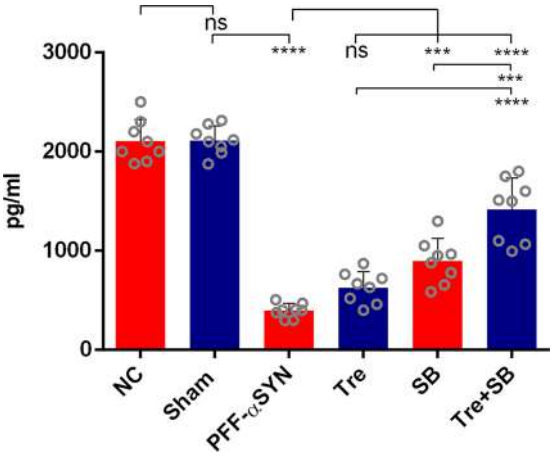

Figure 8. Effect of tre and SB on BDNF levels. Values represent mean ± SD, ****$P \leq 0.0001$ (sham vs PFF α-syn); ns (PFF α-syn vs tre); ***$P \leq 0.001$ (PFF α-syn vs SB); ****$P \leq 0.0001$ (PFF α-syn vs tre +SB); ****$P \leq 0.0001$ (tre+SB vs tre); ***$P \leq 0.001$ (tre+SB vs SB), $F(5,42) = 105.8$, $P < 0.0001$, ns: nonsignificant, NC: normal control.

form, evokes neuronal death. Therefore, we analyzed the mRNA expression level of α-syn in its native form and its effect in the PFF α-syn group and after treatment with tre and SB. The fibrillar form was found to reduce the levels of α-syn mRNA when compared with the sham group (****$P \leq 0.0001$). Quite interestingly, we observed that α-syn expression was significantly improved after treatment with tre and SB alone and with their combination when compared to the group administered with the toxic oligomeric form of α-syn (**$P \leq 0.01$, ****$P \leq 0.0001$, ****$P \leq 0.0001$ respectively). Moreover, the combination group was compared with tre and SB treatments alone and revealed a significant improvement in the α-syn expression level, as ****$P \leq 0.0001$ for both tre+SB vs tre and tre+SB vs SB (Figure 11F).

The cytoskeletal protein MAP-2 stabilizes the microtubule assembly. The progressive loss of DA neurons is due to the formation of cytoplasmic LBs during PD. The alteration in the cellular cytoskeleton and allied aberrant neuronal transport can lead to neuronal loss. The microtubules in neuronal dendrites are stabilized with cytoskelton protein MAP-2, which also mediates for the interaction with neighboring neurons. Hence, we analyzed the levels of MAP-2 mRNA expression in the current study and found that there was a considerable reduction in the MAP-2 expression in the PFF α-syn group (**$P \leq 0.01$), which was efficiently reversed by tre and SB treatment alone and their combination (*$P \leq 0.05$, ****$P \leq 0.0001$, ****$P \leq 0.0001$ respectively). Further, the MAP-2 expression in the combination group was found significantly increased when compared with tre and SB alone (****$P \leq 0.0001$ for both tre+SB vs tre and tre+SB vs SB) (Figure 11G).

Western Blot Analysis. SQSTM1 is a cytoplasmic protein detectable in inclusion bodies of protein aggregates that are responsible for degradation of ubiquitinated substrates. Here, we examined SQSTM1 levels in the SN region of the brain and observed faint bands in the PFF α-syn group which was reversed after tre and SB treatment, where the single treatment of the drugs increased SQSTM1 protein levels and the combination treatment significantly upregulated the SQSTM1 protein level when compared to the PFF α-syn group, which might be attributable to the capacity of tre to increase SQSTM1 levels.[33] Moreover, when the combination group was compared with treatments alone, the SQSTM1 protein level was significantly increased, as *$P \leq 0.05$ for tre+SB vs tre and *$P \leq 0.05$ for tre+SB vs SB (Supplementary Figure 4A,B). The expression level of SQSTM1 correlated with other autophagic flux markers, which limits assessment of the SQSTM1 level in understanding the autophagy mechanism. Moreover, SQSTM1 is degraded by autophagy as well as the proteasome system, and this proteasome inhibition can increase the SQSTM1 level, although proteasome inhibition can increase autophagosome.[34,35] The SQSTM1 contains a domain that can interact with many signaling moieties, which points out its other function. The studies conducted by Abokyi et al. demonstrated that tre treatment in human retinal pigment epithelial cells was found to increase the SQSTM1 level; however, the expression level was much higher when coincubated with chloroquine, indicating the increased synthesis of SQSTM1 by tre.[36] Considering the level of SQSTM1 is not sufficient to assess autophagy, hence in parallel to this, the expression of LC3-II was also checked. Cytosolic LC3-I undergoes post-translational modification from endogenous LC3 which is then converted to LC3-II that is attached to autophagosome membranes.[37] LC3-II (PE-conjugated) has a larger molecular weight than that of LC3-I (16 kDa), which is why on SDS-PAGE, due to its extreme hydrophobicity, LC3-II migrates faster than LC3-I, reaching approximately 15 kDa as seen in the image. Tre and SB are known to upregulate the protein levels of LC3-II,[38,39] which was consistent with our findings where we observed a significant upregulation in tre and SB treatments alone as well as in the combination group, in contrast to that of the disease group (**$P \leq 0.01$, *$P \leq 0.05$, **$P \leq 0.01$, respectively). The increase in the LC3-II protein levels were observed to be statistically similar for the drugs treated alone and in combination (Supplementary Figure 4A,C).

Histopathological Analysis. Along with motor abnormalities observed during the assessment of the behavioral parameters, the PFF α-syn group presented with morphological alterations, particularly in the SN region of the brain. The brain sections stained with H&E revealed the presence of healthy/normal neurons in the SN region in the sham and normal control groups. The ratio of healthy neurons was found

https://doi.org/10.1021/acschemneuro.1c00144
ACS Chem. Neurosci. 2021, 12, 2643−2660

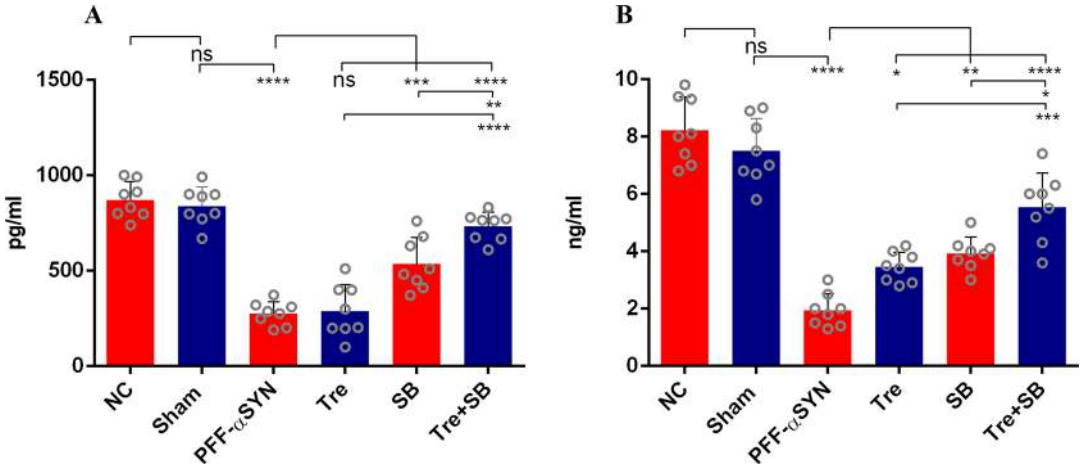

Figure 9. (A) Effect of tre and SB on DA levels in SN. Values represent mean ± SD, ****$P \leq 0.0001$ (sham vs PFF α-syn); ns (PFF α-syn vs tre); ***$P \leq 0.001$ (PFF α-syn vs SB); ****$P \leq 0.0001$ (PFF α-syn vs tre+SB); ****$P \leq 0.0001$ (tre+SB vs tre); **$P \leq 0.01$ (tre+SB vs SB), $F(5,42) = 51.40$, $P < 0.0001$. (B) Striatum DA level. ****$P \leq 0.0001$ (sham vs PFF α-syn); *$P \leq 0.05$ (PFF α-syn vs tre); **$P \leq 0.01$ (PFF α-syn vs SB); ****$P \leq 0.0001$ (PFF α-syn vs tre+SB); ***$P \leq 0.001$ (tre+SB vs tre) *$P \leq 0.05$ (tre+SB vs SB), $F(5,42) = 57.38$, $P < 0.0001$; ns: nonsignificant, NC: normal control.

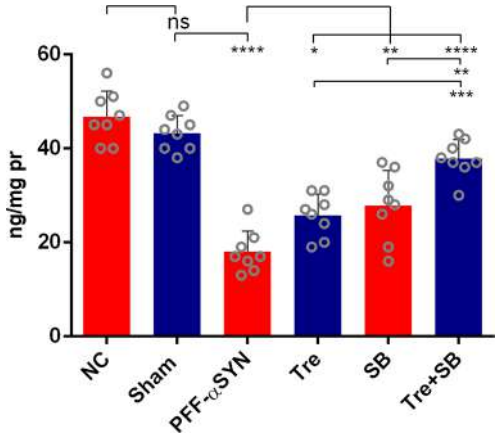

Figure 10. Effect of tre and SB on H3 levels. Values represent mean ± SD, ****$P \leq 0.0001$ (sham vs PFF α-syn); *$P \leq 0.05$ (PFF α-syn vs tre); **$P \leq 0.01$ (PFF α-syn vs SB); ****$P \leq 0.0001$ (PFF α-syn vs tre+SB); ***$P \leq 0.001$ (tre+SB vs tre); **$P \leq 0.01$ (tre+SB vs SB), $F(5,42) = 38.02$, $P < 0.0001$, ns: nonsignificant, NC: normal control.

to be approximately equivalent for both normal and sham control groups. The normal neurons were observed as spherical with a slight oval-shaped nucleus, a nucleolus, and a clear cytoplasm (represented with yellow arrows). On the other hand, the PFF α-syn group had a decreased neuronal density, increased pyknotic and darkly stained neurons, shrunken neurons, and slight vacuolization in the SN region (represented with red arrows). The treatment with tre and SB alone could faintly ameliorate the PFF α-syn induced neuronal pyknosis and loss of neuronal density (*$P \leq 0.05$ for SB; Supplementary Figure 5). However, a significant reduction in the pyknotic neurons and improved neuronal distribution were observed in the combination treatment with tre and SB (**$P \leq 0.01$). Further, when the combination group was compared with treatments alone, the percentage neurodegenerative area tended to decrease significantly with tre (*$P \leq 0.05$, tre+SB vs tre) but not with SB (Figure 12 and Supplementary Figure 5).

Immunofluorescence Analysis. *Estimation of Astrogliosis and Microgliosis.* No significant differences were observed in terms of immunoreactivity for the normal and sham control groups. Thus, only the sham group was kept as the control group. Moreover, from the behavioral, mRNA expression level and histochemical analysis, we found that the animals treated with a combination of tre and SB significantly improved the PD condition. Hence, we chose the combination group for immunolabeling to further confirm its efficacy in ameliorating PD pathology.

Postmortem analysis revealed the importance of microgliosis and astrogliosis in PD. Examining the extent of inflammation in the microglia and astrocytes could provide a better explanation on the severity of PD pathology. Autophagy stimulation and suppression of the hepatic inflammatory chain by tre have attracted the attention of researchers.[40−42] Additionally, the antioxidant and lipid peroxidation activities in tre supplemented with a diet of cow milk were improved.[43,44] Moreover, in a study conducted by Chen et al. on mice models of inflammatory bowel disease induced by TNBS, the SB treatment prevented inflammation and maintained epithelial barrier integrity.[45]

GFAP, a protein mainly known to regulate astrocyte function and morphology, was used as an effective astrogliosis marker, and IBA-1, a microglia specific calcium-binding protein involved in phagocytosis in activated microglia, was used to measure the extent of microgliosis in the PD brain. Quite interestingly, we observed that there was an increase in the number of GFAP cells (green) (**$P \leq 0.01$) and IBA-1 (red) in the PFF α-syn group (*$P \leq 0.05$) and a gradual decrease in the total number of GFAP cells in the treated group with a combination of tre and SB (**$P \leq 0.01$) (Figure 13) and also IBA-1 cells (*$P \leq 0.05$).

Estimation of DA Neuronal Loss. During PD, there is a substantial loss particularly in the TH, the rate limiting enzyme in DA synthesis along with the loss of NeuN. In PD, NeuN is used to estimate the exact loss of nigral DA neurones that can be effectively differentiated from TH loss alone. After performing IFC for the SN region to detect TH and NeuN positive cells, it was observed that the percentage (%) positive cells for TH and NeuN was quite low in the PFF α-syn group which was restored after treatment with the combination of tre and SB (*$P \leq 0.05$) (Figure 14).

https://doi.org/10.1021/acschemneuro.1c00144
ACS Chem. Neurosci. 2021, 12, 2643−2660

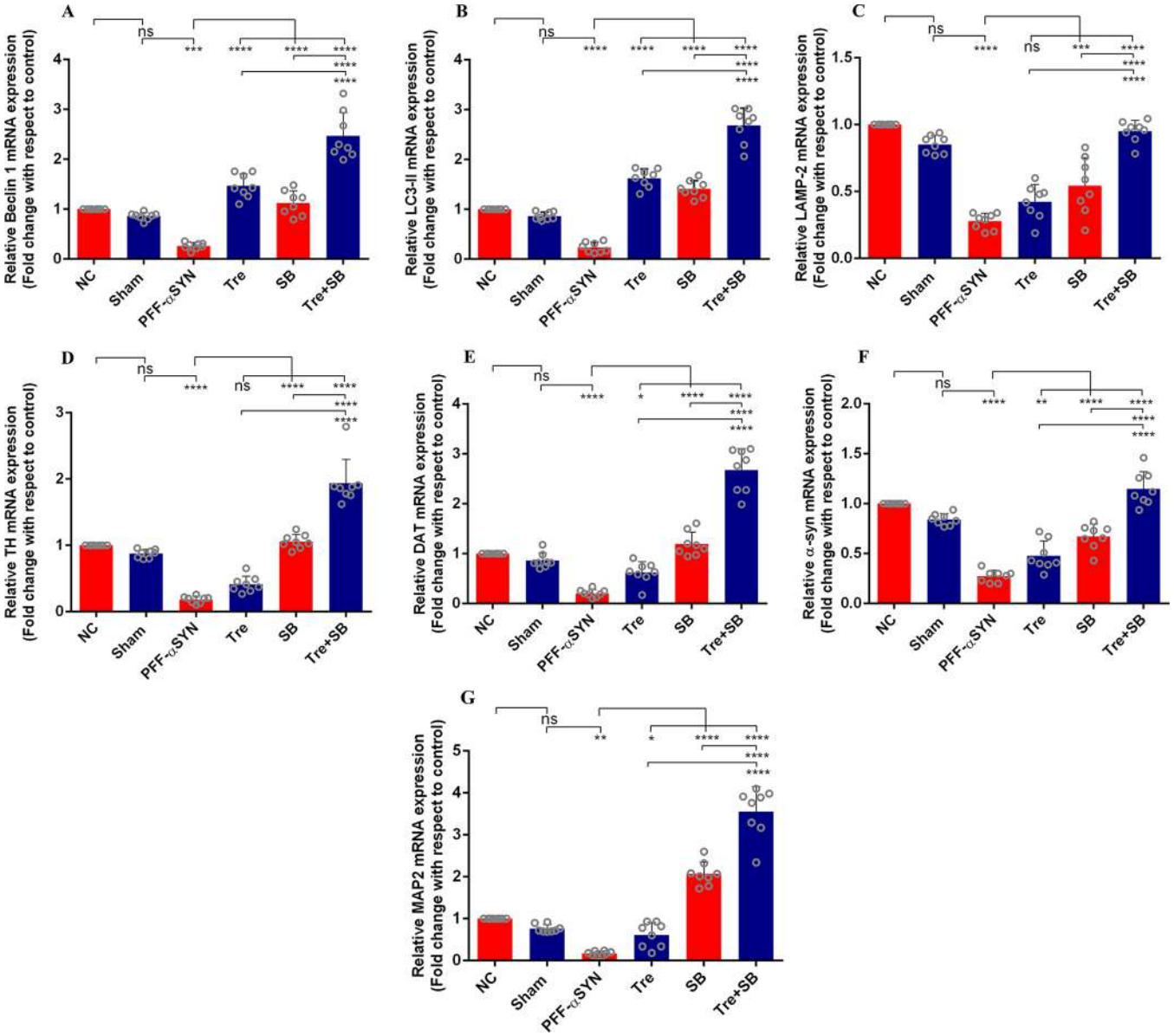

Figure 11. (A) Effect of tre and SB on beclin-1 mRNA expression. Values represent mean ± SD, ***$P \leq 0.001$ (sham vs PFF α-syn); ****$P \leq 0.0001$ (PFF α-syn vs tre); ****$P \leq 0.0001$ (PFF α-syn vs SB); ****$P \leq 0.0001$ (PFF α-syn vs tre+SB); ****$P \leq 0.0001$ (tre+SB vs tre); ****$P \leq 0.0001$ (tre+SB vs SB), $F(5,42) = 73.35$, $P < 0.0001$. (B) LC3-II mRNA expression. Values represent mean ± SD, ****$P \leq 0.0001$ (sham vs PFF α-syn); ****$P \leq 0.0001$ (PFF α-syn vs tre); ****$P \leq 0.0001$ (PFF α-syn vs SB); ****$P \leq 0.0001$ (PFF α-syn vs tre+SB); ****$P \leq 0.0001$ (tre +SB vs tre); ****$P \leq 0.0001$ (tre+SB vs SB), $F(5,42) = 165.7$, $P < 0.0001$. (C) LAMP-2 mRNA expression. Values represent mean ± SD, ****$P \leq 0.0001$ (sham vs PFF α-syn); ns (PFF α-syn vs tre), ***$P \leq 0.001$ (PFF α-syn vs SB), ****$P \leq 0.0001$ (PFF α-syn vs tre+SB); ****$P \leq 0.0001$ (tre+SB vs tre); ****$P \leq 0.0001$ (tre+SB vs SB), $F(5,42) = 57.06$, $P < 0.0001$. (D) TH mRNA expression: Values represent mean ± SD, ****$P \leq 0.0001$ (sham vs PFF α-syn); ns (PFF α-syn vs tre); ****$P \leq 0.0001$ (PFF α-syn vs SB); ****$P \leq 0.0001$ (PFF α-syn vs tre+SB); ****$P \leq 0.0001$ (tre+SB vs tre); ****$P \leq 0.0001$ (tre+SB vs SB), $F(5,42) = 110.6$, $P < 0.0001$. (E) DAT mRNA expression. Values represent mean ± SD, ****$P \leq 0.0001$ (sham vs PFF α-syn); *$P \leq 0.05$ (PFF α-syn vs tre); ****$P \leq 0.0001$ (PFF α-syn vs SB); ****$P \leq 0.0001$ (PFF α-syn vs tre+SB); ****$P \leq 0.0001$ (tre+SB vs tre); ****$P \leq 0.0001$ (tre+SB vs SB), $F(5,42) = 106.8$, $P < 0.0001$. (F) α-syn mRNA expression. Values represent mean ± SD, ****$P \leq 0.0001$ (sham vs PFF α-syn); **$P \leq 0.01$ (PFF α-syn vs tre); ****$P \leq 0.0001$ (PFF α-syn vs SB); ****$P \leq 0.0001$ (PFF α-syn vs tre +SB); ****$P \leq 0.0001$ (tre+SB vs tre); ****$P \leq 0.0001$ (tre+SB vs SB), $F(5,42) = 70.22$, $P < 0.0001$. (G) Effect of tre and SB on MAP-2 mRNA expression. Values represent mean ± SD, **$P \leq 0.01$ (sham vs PFF α-syn); *$P \leq 0.05$ (PFF α-syn vs tre), ****$P \leq 0.0001$ (PFF α-syn vs SB); ****$P \leq 0.0001$ (PFF α-syn vs tre+SB); ****$P \leq 0.0001$ (tre+SB vs tre); ****$P \leq 0.0001$ (tre+SB vs SB), $F(5,42) = 141.1$, $P < 0.0001$, ns: nonsignificant, NC: normal control.

Estimation of Phosphorylated α-Syn (Serine 129). PD pathogenesis undergoes various post-translational modifications to α-syn, one among them is the phosphorylated α-syn (p α-syn) which is known to enhance α-syn toxicity both *in vitro* and *in vivo*. Therefore, we wanted to see whether there is any change in p α-syn levels counterstained with TH before and after treatment. The PFF α-syn group had a high intensity of p α-syn (red) on comparison with the sham group (*$P \leq 0.05$). Conversely, almost no p α-syn signal was detected in the group administered with both tre and SB (*$P \leq 0.05$) with an increased count of positive cells for TH (Figure 15).

https://doi.org/10.1021/acschemneuro.1c00144
ACS Chem. Neurosci. 2021, 12, 2643−2660

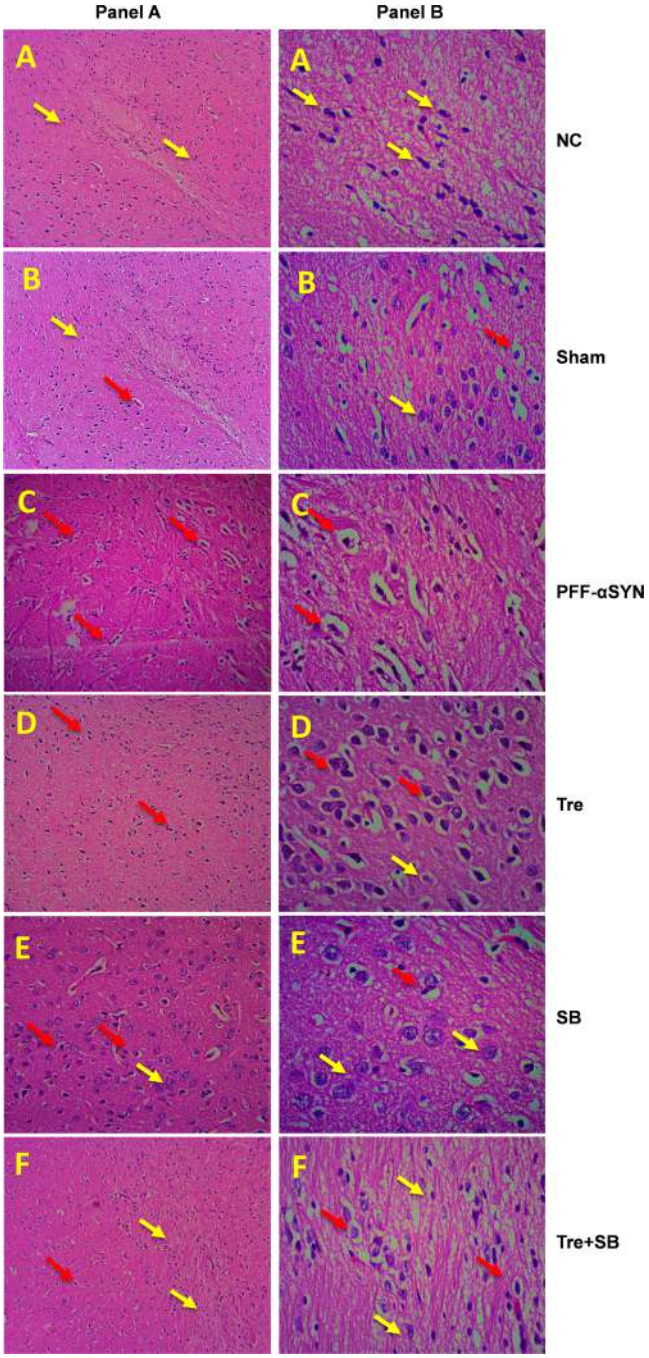

Figure 12. H&E analysis of the SN region of the brain at 10× (A) and 40× magnification (B). As observed in 40× magnification, the figures A and B display the presence of spherical neuronal bodies with a greater density indicated by yellow arrows, C represents darkly stained and shrunken neurones with slight vacuolization, D and E seem to revive the loss of neurones with less darkly stained and shrunken neurones, as indicated by yellow arrows, and F represents a dense population of neurones with a spherical/oval-shaped nucleus indicating the presence of healthy neurones. (A: NC; B: sham; C: PFF-Asyn; D: tre; E: SB; F: tre+SB).

A complete therapeutic cure to halt the pathological progression of PD has time and again failed to reach the market and continues to emerge as a global threat. Symptomatic management with a combination of levodopa and carbidopa is the only successful hope by far. Traditionally, PD was believed to affect motor functions of an individual due to DA neuronal loss, particularly in the SN region of the brain. However, insight into recent research has brought into the limelight certain nonmotor symptoms, mainly cognitive disturbances that might also precede the occurrence of PD. DA neuron loss is likely to occur due to an abnormal misfolding of the oligomeric form of α-syn, notably the PFF form.

The actual causal factor for this misfolding remains largely unknown, but in order to maintain a healthy neuronal environment, removing these misfolded proteins with time is crucial, which throws light on autophagy, a self-conserved mechanism that can eliminate damaged and misfolded proteins governing homeostasis in the body. But as neurodegeneration progresses, autophagy becomes dysfunctional and unable to clear out misfolded proteins; hence, autophagy activation has yielded promising results in several preclinical models of neurodegeneration. During PD, administration of tre to rats has resulted in successful neuroprotection, although the mechanism behind this neuroprotection is surrounded by a lot of controversy. Nevertheless, continuous research has shed some light on the mechanism unravelling a novel direction to neuroprotection elicited by tre. Epigenetic modifications resulting during the pathological progression of PD, notably post-translational histone modifications, have the potential to regulate the expression of autophagy related genes. This theory in itself motivated our current study where we investigated the neuroprotective efficacy of a combination of tre and SB to ameliorate PD pathology in a PFF α-syn model in rats. Tre and SB have been known as a kind of short chain fatty acid (SCFA), which is a byproduct of microbial fermentation. Several previous studies described that treatment of SCFA, for example, SB, or a mixture of SCFA aggravates neuroinflammation and motor deficits in the MPTP mice model and α-syn overexpressing mice model.[46,47] Works by others have suggested the opposite, which revealed that the treatment of tre ameliorated the pathology in the ALS/Huntington mice model.[48,49] However, in the current work, we observed that, as compared to the combination treatment, treatment with tre alone could not ameliorate PD pathology up to a statistically significant level, hinting toward the possibility that its protective effects are not only mediated via SCFA. Tre primarily functions as a protein stabilizer with autophagy activation as its secondary pharmacological function. In a transgenic (tg) mouse model of Huntington's disease, the tre administered orally enhanced motor dysfunction and improved lifespan. With tre administration, superoxide dismutase 1 mutant tg mice had a slightly longer lifetime and improved neuronal survival. In the brains of Parkin−/−/TauVLW mice, phosphorylated tau-positive neuritic plaques and astrogliosis were significantly reduced. Tre inhibited the reduction of striatal DA levels and prevented gliosis in the MPTP mouse model of PD.[50] However, the neuroprotective efficacy of tre to ameliorate PFF α-syn induced PD has not yet been explored, and the results of the present work clearly stated that, as compared to tre alone, its combination with SB elicits a much pronounced neuroprotective efficacy in the PFF α-syn induced rat model of PD.

First, we started by examining a battery of behavioral abnormalities in the PFF α-syn rats and after each of the respective treatments. Based on the results obtained, it was fairly visible that the animals induced with PFF α-syn had significant motor abnormalities both in the rotarod test and NBW test when compared to the control groups. These

https://doi.org/10.1021/acschemneuro.1c00144
ACS Chem. Neurosci. 2021, 12, 2643−2660

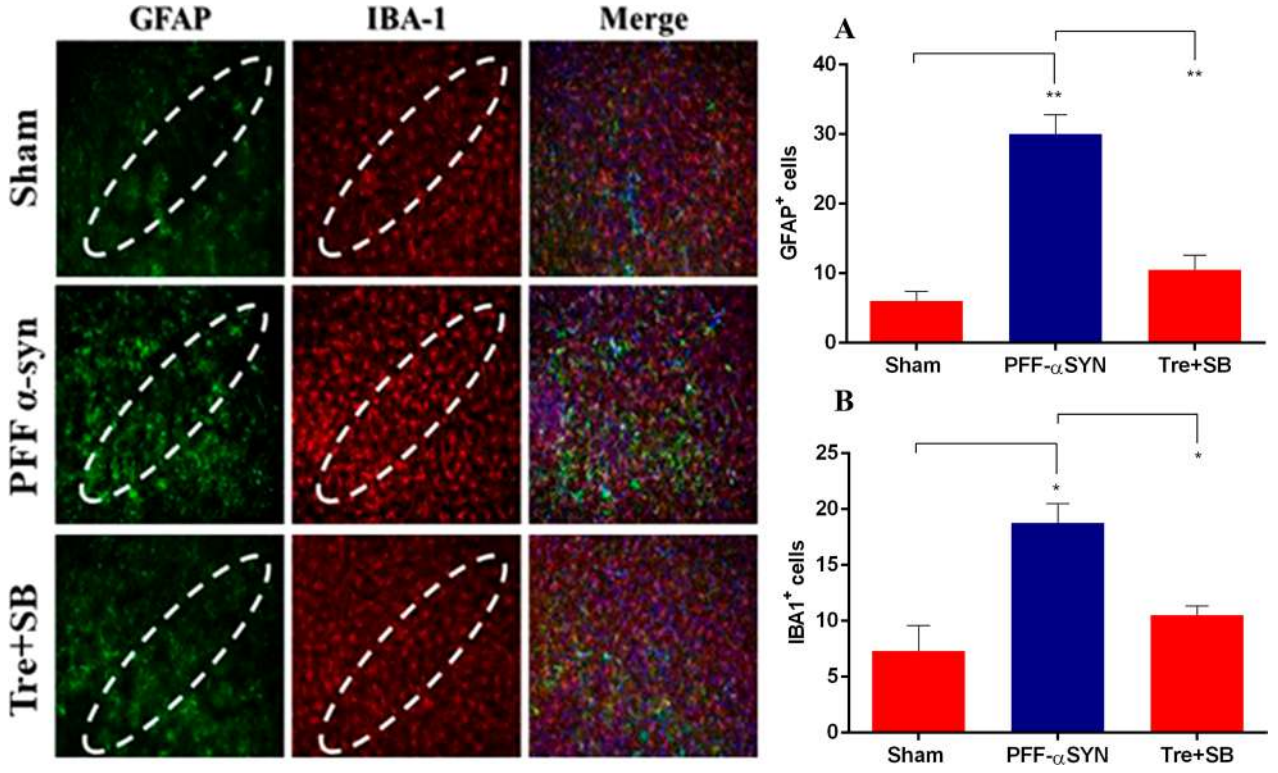

Figure 13. Increased astrogliosis (GFAP, green) and microgliosis (IBA-1, red) in the SN after striatal seeding of PFF α-syn and effective reversal after treatment with tre and SB. Bar graphs represent mean ± SD. (A) GFAP$^+$ cells: $^{**}P \leq 0.01$ (NC vs PFF α-syn); $^{**}P \leq 0.01$ (PFF α-syn vs tre +SB), $F(2,3) = 67.34$, $P = 0.0032$. (B) IBA1$^+$ cells: $^{*}P \leq 0.05$ (NC vs PFF α-syn); $^{*}P \leq 0.05$ (PFF α-syn vs tre+SB), $F(2,3) = 23.36$, $P = 0.0148$, ns: nonsignificant, NC: normal control.

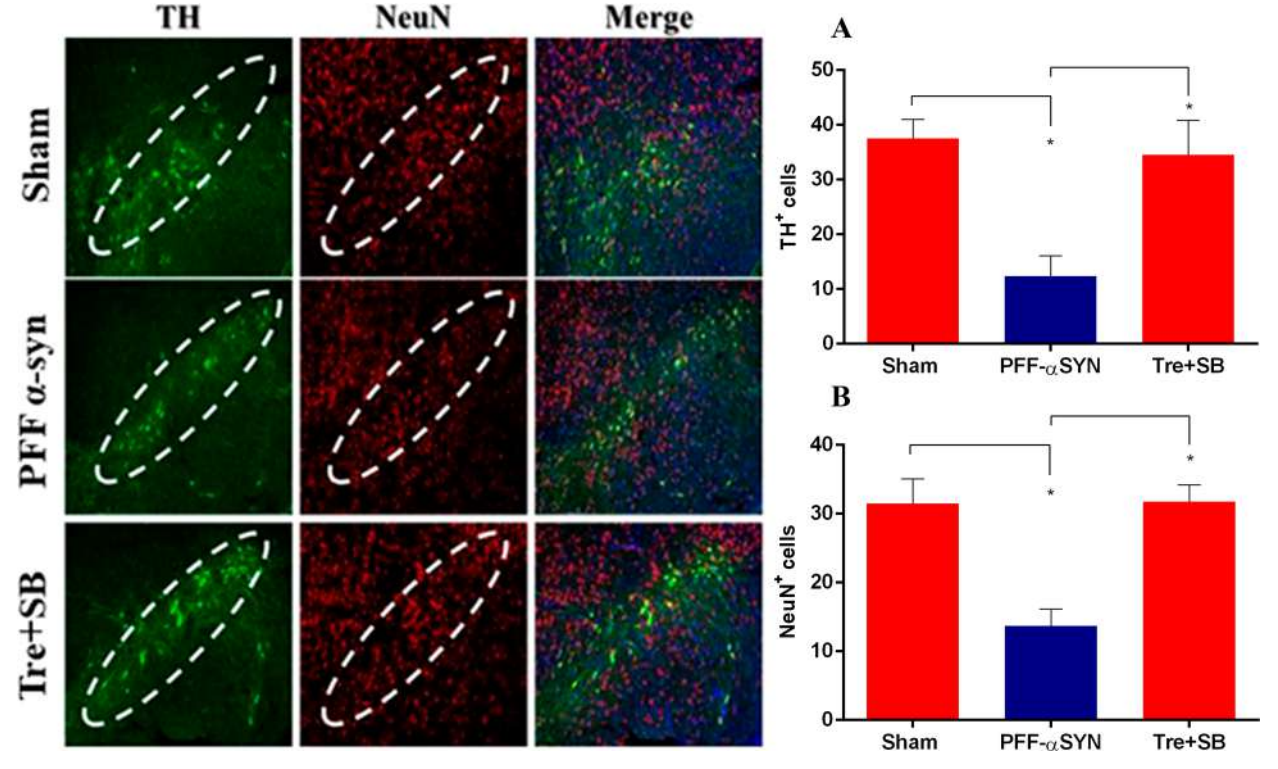

Figure 14. Increased DA neurodegeneration as evidenced after staining with TH (green) and NeuN (red) in the SN after striatal seeding of PFF α-syn and effective reversal after treatment with tre and SB. Bar graphs represent mean ± SD. (A) TH$^+$ cells: $^{*}P \leq 0.05$ (NC vs PFF α-syn); $^{*}P \leq 0.05$ (PFF α-syn vs tre+SB), $F(2,3) = 16.89$, $P = 0.0233$. (B) NeuN$^+$ cells: $^{*}P \leq 0.05$ (NC vs PFF α-syn); $^{*}P \leq 0.05$ (PFF α-syn vs tre+SB), $F(2,3) = 26.33$, $P = 0.0125$, ns: nonsignificant, NC: normal control.

https://doi.org/10.1021/acschemneuro.1c00144
ACS Chem. Neurosci. 2021, 12, 2643−2660

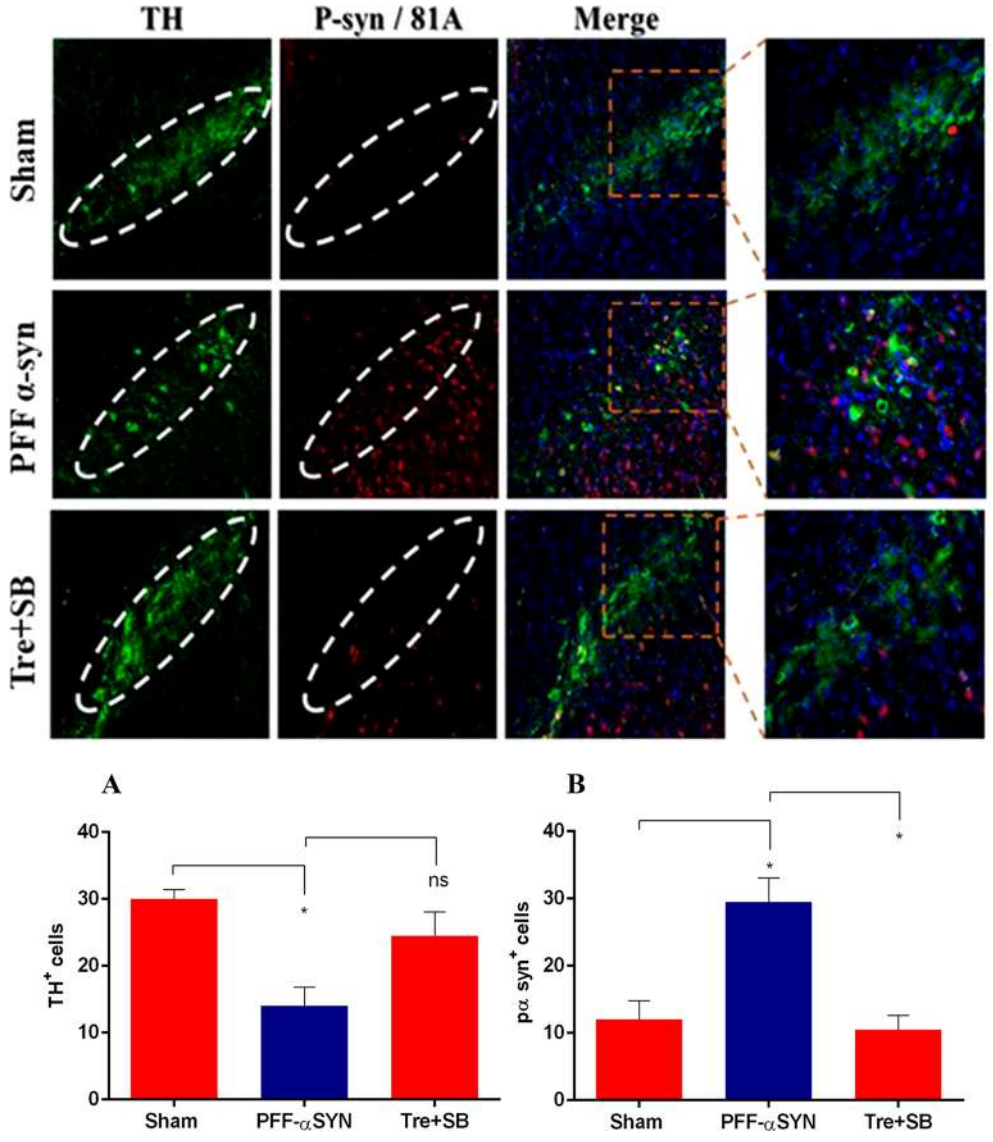

Figure 15. Increased levels of phosphorylated α-syn (S129) (red) and decreased levels of TH (green) in the SN after striatal seeding of PFF α-syn and effective reversal after treatment with tre and SB. Bar graphs represent mean ± SD. (A) TH^+ cells: $^*P \leq 0.05$ (sham vs PFF α-syn); ns (PFF α-syn vs tre+SB), $F(2,3) = 17.62$, $P = 0.0220$. (B) P α-syn^+ cells: $^*P \leq 0.05$ (NC vs PFF α-syn); $^*P \leq 0.05$ (PFF α-syn vs tre+SB), $F(2,3) = 26.78$, $P = 0.0122$, ns: nonsignificant, NC: normal control.

abnormalities were reversed after treatment with a combination of tre and SB. The open field test was used to rule out any locomotor abnormality the animal might be suffering due to induction of the disease and its response after providing the respective treatment. Here, we observed that the disease group had a lower latency of distance traveled as compared to the group treated with the combination of tre and SB. Lastly, we determined any cognitive disturbance that might occur during PD, and for that, we tested the animals using the NOR and NOL test. All the animals injected with PFF α-syn alone were found to have a cognitive discrepancy as compared to the control groups, whereas the treated group both with tre and SB revealed a considerable improvement. For all the tested behavioral parameters, the combination group receiving treatment with both tre and SB had a statistically significant improvement on the behavioral outcome of all the PD induced rats.

Second, we investigated the levels of relevant biochemical markers namely, IL-1, IL-6, TNF-α, CRP, DA, BDNF, and global histone H3 acetylation with available ELISA kits. It was observed that levels of IL-1, IL-6, TNF-α, and CRP considerably upregulated in the PFF α-syn group and significantly improved after treatment with the combination of tre and SB. Likewise, the expression of BDNF, DA, and H3 acetylation downregulated in the PFF α-syn group which significantly upregulated on treatment with the combination of tre and SB.

The analysis of gene expression level of certain genes also revealed similar results, whereby we found that the mRNA expression of genes like beclin-1, LC3-II, LAMP-2, the three most important determinants for the process of autophagy or autophagy induction, considerably downregulated in the PFF α-syn group alone; however, interestingly, the expression level of these genes improved after administration of the combination of tre and SB. Moreover, after the analysis of α-syn, DAT, TH, and MAP-2, we could conclusively state that the treatment group with both tre and SB had a fairly potent

https://doi.org/10.1021/acschemneuro.1c00144
ACS Chem. Neurosci. 2021, 12, 2643−2660

effect even on the expression level of proteins affected most during PD pathology.

Additionally, histopathological analysis of the majorly affected area of the brain during PD, SN revealed heavily degenerated and pyknotic neurones in the group with PFF α-syn alone, which could be reversed after administration of a combination of tre and SB, where it was observed that there was a low pyknotic neuronal count with a low amount of darkly stained neurons.

Lastly, IFC staining for the SN region of the brain exposed improved results with the combination group, for instance, costaining of TH with NeuN showed that the group with PFF α-syn had a lower positive-cell count for TH staining (green) as well as for the NeuN staining (red) on comparison with the sham control group which was reversed on administration with both tre and SB. Similarly, upon counter staining of GFAP (green) with IBA1 (red), we observed that inflammation in the microglia and astrocytes was quite high for the PFF α-syn group and low for the group receiving treatment with both tre and SB. Lastly, we wanted to see if PFF α-syn induction could affect the p α-syn level, and it was seen that there was a considerable upregulation of p α-syn in the PFF α-syn group. However, a significant downregulation of p α-syn was seen in the groups treated with both tre and SB.

CONCLUSION

Neurodegenerative disorders like PD have caused an enormous burden to society as the exact pathogenesis remains elusive. In the current study, we investigated the potency of tre, an autophagy inducer, and SB, a pan HDAC inhibitor, in ameliorating PD pathology exacerbated by PFF α-syn. Although extensive studies are still mandatory to clearly substantiate these findings, preclinical findings in the present study have effectively concluded that tre and SB may prove to be a very powerful combination and can be considered as effective therapeutic candidates for future clinical trials in PD.

MATERIALS AND METHODS

Drugs and Chemicals. Recombinant α-syn (Rpeptide), trehalose (Sigma-Aldrich), sodium butyrate (Cayman chemical), sulphosalicylic acid, Griess reagent, acetylthiocholine iodide, 5,5-dithiobis(2-nitrobenzoic acid) (DTNB), and hematoxylin and eosin (H&E) were purchased from Sigma-Aldrich, USA. TRIzol Reagent was purchased from Invitrogen, USA. Random hexamer, RevertAid Reverse Transcriptase, and 2× Maxima SYBR Green/ROX qPCR Master Mix were acquired from Thermo Fischer, USA. Interleukin-1 (IL-1), interleukin-6 (IL-6), tumor necrosis factor alpha (TNF-α), and brain derived neurotrophic factor (BDNF) ELISA kits were purchased from Boster Biotech, USA. C-reactive protein (CRP) ELISA kit was purchased from R&D Systems. Dopamine (DA) ELISA kit was procured from USCN Life Sciences, Houston, USA. Global histone H3 acetylation kit was procured from Epigentek. Primers: Microtubule-associated protein 1A/1B-light chain 3 phosphatidylethanolamine conjugate (LC3-II), beclin 1, lysosome-associated membrane protein-2 (LAMP-2), dopamine active transporter (DAT), tyrosine hydroxylase (TH), α-syn, microtubule associated protein-2 (MAP 2), and glyceraldehyde 3 phosphate dehydrogenase (GAPDH) were acquired from Imperial Life Sciences Limited. Additional reagents/chemicals were purchased from SRL and CDH, India, and all other biological diluents used in the study were freshly prepared prior to use.

Antibodies for the Current Study. Primary antibodies used in the present study are mouse anti-α-synuclein, pS129 (1:2000) (ab27766; Abcam), chicken anti-Glial fibrillary acidic protein (GFAP, 1:4000) (ab4674, Abcam), mouse anti-TH (1:2000) (MA318, Millipore), mouse antineuronal nuclear protein (NeuN, 1:2000) (MAB377, Millipore), rabbit anti-ionized calcium binding adaptor molecule 1 (Iba1, 1:4000) (019-19741, Wako), 4′,6-diamidino-2-phenylindole dihydrochloride (DAPI, D1306, Thermo Fisher, 1:10000). Secondary antibodies used include the following: Anti-chicken (CF-488, Biotium), anti-rabbit (CF-568 and 594, Biotium), anti-mouse (CF-488, Biotium), anti-LC3 antibody (Sigma-Aldrich), anti-SQSTM1 antibody (procured from Thermo Fisher Scientific), and anti-β-actin antibody and secondary goat antirabbit IgG antibody (Sigma-Aldrich).

Animals. Male wistar rats (200−250 g, 8−10 weeks old) were housed at the central animal facility, BITS-Pilani, Pilani campus with standard laboratory conditions (temperature: 20−22 °C, humidity: 65%) on a 12:12 h light:dark cycle with food and water ad libidum. Institutional Animal Ethics Committee (IAEC) - BITS-Pilani, Pilani Campus, Rajasthan approved all experiments and sample collection (approved protocol no.: IAEC/RES/24/14).

Preparation of PFF α-Syn. Briefly, recombinant human α-syn (1 mg) commercially available was obtained from Rpeptide and rapidly thawed and resuspended in distilled water to a final concentration of 1000 μL. The resuspended vial was then centrifuged at 100,000*g* for 60 min in 4 °C to pellet any aggregated material. Following which the tube was placed in a thermomixer that was maintained at 37 °C (this avoids condensation, which will affect the concentration of fibril). The tube was then shaken for 7 days at 1000 rotation per minute (rpm) along with probe sonication for 30 s (0.5 s pulse on and off). The solution in the tube appeared turbid after day 7. The final solution after shaking for 7 days was divided in 20 μL aliquots into sterile microcentrifuge tubes and stored at −80 °C for further use.[51] Confirmation of the formation of PFF was done by Coomassie staining.

Sedimentation Assay for PFF α-Syn. 20 μL of PFFs was pipetted into a tube that was centrifuged at 100,000*g* for 60 min at room temperature. 20 μL of supernatant was removed and transferred to a new tube to which 20 μL of 2× Laemmli buffer was added. 20 μL of PBS was used to suspend the pellet and centrifuged again at 100,000*g* for 30 min. The supernatant was removed. To this fraction, the pellet was suspended in 20 μL of PBS, and 20 μL of 2× Laemmli buffer was added. 15 μL of the supernatant from the first step and pellet from the last step was added onto a 4−20% (wt/vol) acrylamide gel with a 15-well comb to perform Coomassie staining and destaining. Approximately equivalent amounts of α-syn should run above the 15 kDa marker in the supernatant and pellet, as is observed in the Supplementary Figure 2.

Stereotaxic Injection of PFF α-Syn. Eight-week-old wistar rats were deeply anesthetized with 4% chloral hydrate solution. PBS in the sham control group and PFF α-syn (pelleted form) in the disease group (5 μg) were unilaterally injected into the striatum at two points (2.5 μL per hemisphere at 0.5 μL/min) using the coordinates: anteroposterior (AP): +0.2 mm, mediolateral (ML): +2.0 mm, dorsoventral (DV): +2.8 mm and AP = +1.0 mm, ML = +1.5 mm, DV= −2.8 mm from bregma.[51] After the injection, the needle was kept as such for next 5 min for complete absorption of the solution. PFF α-syn was proven to inflict PD pathology post-6 months after its seeding.[51] Treatment with tre and SB was initiated thereafter.

Experimental Protocol. Each group comprised of 8 animals with 6 groups, as described in Table 1. Twenty-8 days treatment with tre and SB were initiated by freshly preparing everyday by dissolving in normal saline, followed by vortexing before administration. The dose for SB was selected based on the studies conducted in our lab previously,[27] whereas the dose of tre for neuroprotective efficacy was selected from literature available to date.[19−21]

Behavioral Parameters Assessment. *Rotarod Test.* The rotarod test is generally used to access the motor performance of the rodents and is a well-accepted model for assessing the extent of PD neuronal degeneration. As the first symptom of PD is motor imbalance, the rotarod test is always the first choice of any researcher for analyzing PD pathology. Briefly, each animal was allowed to move on a rotating rod at an initial rpm of 5 which was progressively increased to 15 rpm. The ability to hold on to the rotating rod even at

https://doi.org/10.1021/acschemneuro.1c00144
ACS Chem. Neurosci. 2021, 12, 2643−2660

Table 1. Experimental Groups Division with Their Respective Treatment

group no.	group	treatment
1	normal control	the animals without any infusion into the striatum
2	sham control	animals were infused with PBS in the striatum
3	PFF α-syn	animals were infused with PFF α-syn intrastriatally
4	tre, 4 g/kg	PFF α-syn animals were treated with tre 4 g/kg, orally
5	SB, 300 mg/kg	PFF α-syn animals were treated with SB 300 mg/kg, orally
6	tre and SB	PFF α-syn animals were treated with tre (2 g/kg) and SB (150 mg/kg), orally

high speed was considered as the normal motor functionality of the rodent. The time to fall (in seconds) was recorded for each animal.[52]

Open Field Test. This test is mainly used to access the locomotor activity, anxiety, and willingness of rodents to explore novel environments. Originally developed by Calvin S. Hall, the principle of the open field test is to rule out the anxious and exploratory behavior of the rodents. During PD, immobility is the first symptom that is normally seen in most of the cases along with the occurrence of anxiety eventually. Hence, decreased mobility with increased anxiety was considered as a parameter to access the severity of PD progression.[53] Briefly, the apparatus consisted of an open field with a wall consisting of grid and square crossings where the rodents were placed in the arena for a period of 15 min, and total distance traveled by each animal was recorded.[54]

NBW Test. The rationale of this test is to assess the time traversed by the animal to move across a thin beam from one end to other end, consisting of a safe platform. The number of paw slips during the process was also recorded.[55] The apparatus was comprised of a thin beam held up 1 m above the ground. The black colored platform was provided with a cushion and the narrow beam placed freely in this cushion. Each animal was allotted 60 s and a maximum of 5 foot slips, and the time taken to move across the beam along with the total number of foot slips were recorded manually.[52]

Novel Object Location and Recognition Test. Cognitive dysfunction is one of the major nonmotor symptoms occurring during late or early PD. The NOR and NOL test is used to rule out the cognitive anomaly of the rodent. The test is comprised of four steps: habituation, training, novel object, and novel location recognition test. Briefly, in the habituation step, the rat is freely allowed to explore in an open field area for a period of 15 min in the absence of objects on the first day. The following day, that is, in the training phase, the rats were presented with two similar looking objects in the same open field and allowed to explore for a period of 5 min. Post-24 h, the animal was presented with one similar object and a novel object,[56] following which the animal was again placed in the same arena with a similar object along with a novel object and a novel location. The duration of the animal to explore the novel object and the novel location was recorded for a period of 5 min[57] and was considered as a measure of extent of cognitive damage.

Assessment of Biochemical Parameters. *Hippocampus/SN Homogenate Preparation.* Decapitation was employed to sacrifice the animals following which the desired region of the brain, that is, hippocampus/SN, was isolated and washed with ice-cold sodium chloride (0.9% w/v). Afterward the parts were homogenized with ice-cold PBS (0.1M, pH 7.4) with 10 times (w/v) volume of the weight of the tissue. The homogenate was centrifuged at 12,000*g* for 15 min at 4 °C, and the supernatant obtained was divided into aliquots and utilized for biochemical estimations.

Protein Estimation. Brain hippocampus/SN protein level was assessed by the Lowry method using bovine serum albumin (1 mg/mL) as a standard.[58]

Estimation of Pro-inflammatory Cytokine TNF-α, IL-1, and IL-6 Levels. Neuroinflammatory markers like TNF-α, IL-1, and IL-6 in the hippocampal and the nigral homogenate were estimated using an ELISA kit as per directions from manufacturer. The values were represented as pg/mL of protein.

Estimation of CRP Level. The CRP level was measured in the striatum homogenate as per the specifications given by the procured ELISA kit.

Estimation of BDNF Level. The BDNF level was assessed in SN homogenates with a commercially available ELISA kit as per the instructions from manufacturer.

Estimation of DA Level. The DA level was estimated in SN as well as the striatum homogenates by using a commercially available ELISA kit as per the instructions from manufacturer.

Estimation of Global Histone H3 Acetylation Level. Global Histone H3 Acetylation EpiQuik Assay Kit was used to determine global histone H3 acetylation level as per instruction from manufacturer.

Ribonucleic Acid (RNA) Isolation. TRIzol Reagent (Invitrogen, 15596018) was used to extract the total RNA from the brain homogenate. Synthesis of cDNA (cDNA) was carried out using RevertAid Reverse Transcriptase (Thermo Fisher, EP0441) along with Random hexamer (Thermo Fisher, SO142).

Real-Time Quantitative Polymerase Chain Reaction (qPCR). The CFX Connect Optics Module (Bio-Rad) was used for qPCR assays. 2× Maxima SYBR Green/ROX qPCR Master Mix (Thermo Fisher, K0221) with specific primers was used for amplification according to manufacturer's instructions (Table 2). The conditions for the PCR were 95 °C (10 min), 40 cycles of 95 °C (15 s), 60 °C (30 s), and 72 °C for (30 s). The $2^{-\Delta\Delta CT}$ method was employed for calculating the relative mRNA expression level.[59]

Western Blot Analysis. Total protein was extracted from the SN by using RIPA buffer that contained phosphatase and protease inhibitors. Equal amounts of lysates were electrophoretically separated by SDS-PAGE gel and transferred onto a nitrocellulose membrane. The blot was probed overnight with primary antibodies, SQSTM1 antibody (Thermo Fisher Scientific), anti-LC3 (Sigma-Aldrich), and anti-β-actin (Sigma-Aldrich) at 4 °C. Corresponding HRP-labeled secondary antibody (goat antirabbit IgG antibody, Sigma-Aldrich) was used, and the signals were visualized using an ECL kit (Thermo Fisher Scientific).

Assessment of Histopathological Changes. A 10% v/v formalin was used as a fixing immersion median after rapid removal of the brains. Paraffin wax was utilized for embedding the brain by

Table 2. Primer Sequences for *In Vivo* Experiments

gene	forward primer	reverse primer
beclin 1	AGCTGCCGTTATACTGTTCTG	ACTGCCTCCTGTGTCTTCAATCTT
LC3-II	GATGTCCGACTTATTCGAGAGC	TTGAGCTGTAAGCGCCTTCTA
LAMP-2	AGCCCCAAACAGCTCAACTT	TATGATGGCGCTTGAGACCA
TH	AGGGCTAAATACGGCTGCTC	CAGCTGCTTCACAGACCCAT
DAT	GCTGCGTCACTGGCTGTTGC	CTGTCCCCGCTGTTGTGAGGT
α-syn	GAGGGAGTCGTTCATGGAGT	CATTTGTCACTTGCTCTTTGG
MAP-2	CGGAAAACCACAGCAGCAAG	ACTTTGGAGGAGTGCGGATG
GAPDH	AGGTCGGTGTGAACGGATTT	TTCCCGTTGATGACCAGCTT

https://doi.org/10.1021/acschemneuro.1c00144
ACS Chem. Neurosci. 2021, 12, 2643−2660

cutting into 5 μm-thick sections and then rehydrated with standard steps. H&E stain was then used to stain these sections along with dehydration combined with clearing and coverslipping. The SN region was analyzed with Optika TCB5 microscope (Optika Research Microscope, Italy) at objective magnifications of 10× and 40×. Photomicrographs of H&E stained sections were imported to ImageJ software (NIH-sponsored public domain image analysis software) and analyzed. Neurons with degenerating characters were calculated using the ImageJ cell counter and represented as the percentage of degenerating neurons.

Immunofluorescence Analysis of Brain Tissue. Briefly, the rats were overdosed with pentobarbital (50 mg/kg) to anesthetize and perfused with heparinized saline and then 10% paraformaldehyde (PFA) using Gilson Minipuls 2. After isolation, the brain was stored in PFA overnight and transferred to 20% sucrose solution for cryoprotection thereafter. After 3 days, the brain tissues, specifically the SN region, were sectioned into 50 μm-thick sections with a Leica sliding microtome, collected in PBS, and transferred in antifreezing solution until further processed for immunofluorecence. The sections were then washed in 0.1 M PBS to remove the freezing solution and then incubated with blocking buffer, followed by incubation with necessary primary antibodies at 4°C. PBS was then used to wash the sections followed by incubation with a secondary antibody and staining the nuclei with DAPI. Finally, the sections were visualized under an Invitrogen EVOS M7000 imaging system.

Statistical Analysis. Results expressed as mean ± SD. A statistical graph pad prism software (version 6.01 and 8.4.3) was used to investigate the significance range of the behavioral and biochemical parameters by one-way analysis of variance followed by Tukey's post hoc test. Histological and immunofluorescence photomicrographs were measured using ImageJ software.

■ ASSOCIATED CONTENT

Supporting Information

The Supporting Information is available free of charge at https://pubs.acs.org/doi/10.1021/acschemneuro.1c00144.

Validation of intrastriatal coordinates; sedimentation assay for PFF fibril; quantified data for the novel object recognition and location tests along with discrimination index; Western blots; and quantified data for the histochemical image (PDF)

■ AUTHOR INFORMATION

Corresponding Author

Rajeev Taliyan − *Neuropsychopharmacology Division, Department of Pharmacy, Birla Institute of Technology and Science Pilani, 333031 Pilani, Rajasthan, India;* orcid.org/0000-0003-2147-2990; Phone: (+91) 8769196560; Email: taliyanraja@gmail.com

Authors

Violina Kakoty − *Neuropsychopharmacology Division, Department of Pharmacy, Birla Institute of Technology and Science Pilani, 333031 Pilani, Rajasthan, India;* orcid.org/0000-0001-8366-8142

Sarathlal K C − *Neuropsychopharmacology Division, Department of Pharmacy, Birla Institute of Technology and Science Pilani, 333031 Pilani, Rajasthan, India;* orcid.org/0000-0003-2297-5258

Sunil Kumar Dubey − *Department of Pharmacy, Birla Institute of Technology and Science Pilani, 333031 Pilani, Rajasthan, India;* orcid.org/0000-0002-7554-3232

Chih-Hao Yang − *Department of Pharmacology, Taipei Medical University, Taipei 110, Taiwan*

Complete contact information is available at: https://pubs.acs.org/10.1021/acschemneuro.1c00144

Author Contributions

V.K., R.T., S.K.D., C.H.Y. designed the current research work. V.K. and S.K.C. performed experiments, analyzed and interpreted the data, and wrote the manuscript. V.K. and C.H.Y. analyzed the histochemical and immunofluorescence results. R.T. approved the final version of the manuscript.

Notes

The authors declare no competing financial interest.

■ ACKNOWLEDGMENTS

Authors acknowledge the support from Birla Institute of Technology and Science (BITS)-Pilani, Pilani Campus Rajasthan, India, and Taipei Medical University, Taipei, Taiwan.

■ ABBREVIATIONS USED

AD, Alzheimer's disease
BDNF, brain derived neurotrophic factor
cDNA, complementary DNA
CMA, chaperone-mediated autophagy
CPU, caudate/putamen
CRP, C-reactive protein
DA, dopamine
DAT, dopamine active transporter
DOPAC, 3,4-dihydroxyphenylacetic acid
GAPDH, glyceraldehyde 3-phosphate dehydrogenase
GFAP, glial fibrillary acidic protein
h, hour
H&E, hematoxylin & eosin
HDACis, histone deacetylase inhibitors
HVA, homovanillic acid
IBA-1, ionized calcium binding adaptor molecule 1
IFC, immunofluorescence
IL-1, interleukin-1
IL-6, interleukin-6
kDa, kilodalton
kg, kilogram
LAMP-2, lysosome-associated membrane protein 2
LBs, lewy bodies
LC3-II, microtubule-associated protein 1A/1B-light chain 3-phosphatidylethanolamine conjugate
m, meter
MAP-2, microtubule associated protein-2
mg, milligram
min, minute
mL, milliliter
mm, millimeter
MPTP, 1-methyl-4-phenyl-1,2,3,6-tetrahydropyridine
mRNA, messenger ribonucleic acid
NaCl, sodium chloride
NBW, narrow beam walk
NC, normal control
NeuN, neuronal nuclear protein
NOL, novel object location
NOR, novel object recognition
ns, nonsignificant
p α-syn, phosphorylated α-syn (serine 129)
PBS, phosphate buffer saline
PD, Parkinson's disease
PDD, Parkinson's disease dementia

PFA, paraformaldehyde
PFF, lreformed fibrillar form
qPCR, quantitative polymerase chain reaction
RNA, ribonucleic acid
RPM, rotation per minute
RIPA, radioimmunoprecipitation assay buffer
SB, Sodium butyrate
sec, second
SnPC, substantia nigra pars compacta
Tg, transgenic
TH, tyrosine hydroxylase
TNF-α, tumour necrosis factor alpha
Tre, trehalose
α-syn, alpha-synuclein
μm, micrometer
°C, degree Celsius
μL, microliter
%, percentage

REFERENCES

(1) Pringsheim, T., Jette, N., Frolkis, A., and Steeves, T. D. L. (2014) The Prevalence of Parkinson's Disease: A Systematic Review and Meta-Analysis. *Mov. Disord. 29* (13), 1583−1590.

(2) Parkinson, J. (2002) An Essay on the Shaking Palsy. *J. Neuropsychiatry Clin. Neurosci. 14* (2), 223−236.

(3) El-Agnaf, O. M. A., Salem, S. A., Paleologou, K. E., Cooper, L. J., Fullwood, N. J., Gibson, M. J., Curran, M. D., Court, J. A., Mann, D. M. A., Ikeda, S.-I., et al. (2003) α-Synuclein Implicated in Parkinson's Disease Is Present in Extracellular Biological Fluids, Including Human Plasma. *FASEB J. 17* (13), 1−16.

(4) Irwin, D. J., Lee, V. M.-Y., and Trojanowski, J. Q. (2013) Parkinson's Disease Dementia: Convergence of α -Synuclein, Tau and Amyloid- β Pathologies. *Nat. Rev. Neurosci. 14* (9), 626.

(5) Poewe, W., Seppi, K., Tanner, C. M., Halliday, G. M., Brundin, P., Volkmann, J., Schrag, A.-E., and Lang, A. E. (2017) Parkinson Disease. *Nat. Rev. Dis. Prim. 3*, 17013.

(6) Rodrigues e Silva, A. M., Geldsetzer, F., Holdorff, B., Kielhorn, F. W., Balzer-Geldsetzer, M., Oertel, W. H., Hurtig, H., and Dodel, R. (2010) Who Was the Man Who Discovered the "Lewy Bodies"? *Mov. Disord. 25* (12), 1765−1773.

(7) Spillantini, M. G., Schmidt, M. L., Lee, V. M.-Y., Trojanowski, J. Q., Jakes, R., and Goedert, M. (1997) α -Synuclein in Lewy Bodies. *Nature 388* (6645), 839−840.

(8) Maroteaux, L., Campanelli, J. T., and Scheller, R. H. (1988) Synuclein: A Neuron-Specific Protein Localized to the Nucleus and Presynaptic Nerve Terminal. *J. Neurosci. 8* (8), 2804−2815.

(9) Dauer, W., and Przedborski, S. (2003) Parkinson's Disease: Mechanisms and Models. *Neuron 39* (6), 889−909.

(10) Beach, T. G., Adler, C. H., Lue, L., Sue, L. I., Bachalakuri, J., Henry-Watson, J., Sasse, J., Boyer, S., Shirohi, S., Brooks, R., et al. (2009) Unified Staging System for Lewy Body Disorders: Correlation with Nigrostriatal Degeneration, Cognitive Impairment and Motor Dysfunction. *Acta Neuropathol. 117* (6), 613−634.

(11) Luk, K. C., Kehm, V. M., Zhang, B., O'Brien, P., Trojanowski, J. Q., and Lee, V. M. Y. (2012) Intracerebral Inoculation of Pathological α -Synuclein Initiates a Rapidly Progressive Neurodegenerative α -Synucleinopathy in Mice. *J. Exp. Med. 209* (5), 975−986.

(12) Cuervo, A. M., Stefanis, L., Fredenburg, R., Lansbury, P. T., and Sulzer, D. (2004) Impaired Degradation of Mutant α -Synuclein by Chaperone-Mediated Autophagy. *Science (Washington, DC, U. S.) 305* (5688), 1292−1295.

(13) Spencer, B., Potkar, R., Trejo, M., Rockenstein, E., Patrick, C., Gindi, R., Adame, A., Wyss-Coray, T., and Masliah, E. (2009) Beclin 1 Gene Transfer Activates Autophagy and Ameliorates the Neurodegenerative Pathology in α -Synuclein Models of Parkinson's and Lewy Body Diseases. *J. Neurosci. 29* (43), 13578−13588.

(14) Felice, V. D., Quigley, E. M., Sullivan, A. M., O'Keeffe, G. W., and O'Mahony, S. M. (2016) Microbiota-Gut-Brain Signalling in Parkinson's Disease: Implications for Non-Motor Symptoms. *Parkinsonism Relat. Disord. 27*, 1−8.

(15) Tanji, K., Miki, Y., Maruyama, A., Mimura, J., Matsumiya, T., Mori, F., Imaizumi, T., Itoh, K., and Wakabayashi, K. (2015) Trehalose Intake Induces Chaperone Molecules along with Autophagy in a Mouse Model of Lewy Body Disease. *Biochem. Biophys. Res. Commun. 465* (4), 746−752.

(16) Martano, G., Gerosa, L., Prada, I., Garrone, G., Krogh, V., Verderio, C., and Passafaro, M. (2017) Biosynthesis of Astrocytic Trehalose Regulates Neuronal Arborization in Hippocampal Neurons. *ACS Chem. Neurosci. 8* (9), 1865−1872.

(17) Béranger, F., Crozet, C., Goldsborough, A., and Lehmann, S. (2008) Trehalose Impairs Aggregation of PrPSc Molecules and Protects Prion-Infected Cells against Oxidative Damage. *Biochem. Biophys. Res. Commun. 374* (1), 44−48.

(18) Casarejos, M. J., Solano, R. M., Gomez, A., Perucho, J., De Yébenes, J. G., and Mena, M. A. (2011) The Accumulation of Neurotoxic Proteins, Induced by Proteasome Inhibition, Is Reverted by Trehalose, an Enhancer of Autophagy, in Human Neuroblastoma Cells. *Neurochem. Int. 58* (4), 512−520.

(19) Ferguson, S. A., Law, C. D., and Sarkar, S. (2015) Chronic MPTP Treatment Produces Hyperactivity in Male Mice Which Is Not Alleviated by Concurrent Trehalose Treatment. *Behav. Brain Res. 292*, 68−78.

(20) Sarkar, S., Chigurupati, S., Raymick, J., Mann, D., Bowyer, J. F., Schmitt, T., Beger, R. D., Hanig, J. P., Schmued, L. C., and Paule, M. G. (2014) Neuroprotective Effect of the Chemical Chaperone, Trehalose in a Chronic MPTP-Induced Parkinson's Disease Mouse Model. *NeuroToxicology 44*, 250−262.

(21) He, Q., Koprich, J. B., Wang, Y., Yu, W., Xiao, B., Brotchie, J. M., and Wang, J. (2016) Treatment with Trehalose Prevents Behavioral and Neurochemical Deficits Produced in an AAV α -Synuclein Rat Model of Parkinson's Disease. *Mol. Neurobiol. 53* (4), 2258−2268.

(22) Füllgrabe, J., Lynch-Day, M. A., Heldring, N., Li, W., Struijk, R. B., Ma, Q., Hermanson, O., Rosenfeld, M. G., Klionsky, D. J., and Joseph, B. (2013) The Histone H4 Lysine 16 Acetyltransferase HMOF Regulates the Outcome of Autophagy. *Nature 500* (7463), 468−471.

(23) Wend, P., Fang, L., Zhu, Q., Schipper, J. H., Loddenkemper, C., Kosel, F., Brinkmann, V., Eckert, K., Hindersin, S., Holland, J. D., et al. (2013) Wnt/ β -Catenin Signalling Induces MLL to Create Epigenetic Changes in Salivary Gland Tumours. *EMBO J. 32* (14), 1977−1989.

(24) Schotta, G., Lachner, M., Sarma, K., Ebert, A., Sengupta, R., Reuter, G., Reinberg, D., and Jenuwein, T. (2004) A Silencing Pathway to Induce H3-K9 and H4-K20 Trimethylation at Constitutive Heterochromatin. *Genes Dev. 18* (11), 1251−1262.

(25) Marques, S., and Outeiro, T. F. Epigenetics in Parkinson's and Alzheimer's Diseases. (2013) In *Epigenetics: Development and Disease*, pp 507−525, Springer, Dordrecht.

(26) Monti, B., Gatta, V., Piretti, F., Raffaelli, S. S., Virgili, M., and Contestabile, A. (2010) Valproic Acid Is Neuroprotective in the Rotenone Rat Model of Parkinson's Disease: Involvement of α -Synuclein. *Neurotoxic. Res. 17* (2), 130−141.

(27) Sharma, S., Taliyan, R., and Singh, S. (2015) Beneficial Effects of Sodium Butyrate in 6-OHDA Induced Neurotoxicity and Behavioral Abnormalities: Modulation of Histone Deacetylase Activity. *Behav. Brain Res. 291*, 306−314.

(28) Siuda, J., Patalong-Ogiewa, M., Zmuda, W., Targosz-Gajniak, M., Niewiadomska, E., Matuszek, I., Jedrzejowska-Szypułka, H., and Rudzinska-Bar, M. (2017) Cognitive Impairment and BDNF Serum Levels. *Neurol. Neurochir. Pol. 51* (1), 24−32.

(29) Kontopoulos, E., Parvin, J. D., and Feany, M. B. (2006) α -Synuclein Acts in the Nucleus to Inhibit Histone Acetylation and Promote Neurotoxicity. *Hum. Mol. Genet. 15* (20), 3012−3023.

https://doi.org/10.1021/acschemneuro.1c00144
ACS Chem. Neurosci. 2021, 12, 2643−2660

(30) Xilouri, M., Vogiatzi, T., Vekrellis, K., Park, D., and Stefanis, L. (2009) Abberant α -Synuclein Confers Toxicity to Neurons in Part through Inhibition of Chaperone-Mediated Autophagy. *PLoS One 4* (5), e5515.
(31) Higashi, S., Moore, D. J., Minegishi, M., Kasanuki, K., Fujishiro, H., Kabuta, T., Togo, T., Katsuse, O., Uchikado, H., Furukawa, Y., et al. (2011) Localization of MAP1-LC3 in Vulnerable Neurons and Lewy Bodies in Brains of Patients with Dementia with Lewy Bodies. *J. Neuropathol. Exp. Neurol. 70* (4), 264−280.
(32) Blanchard-Fillion, B., Souza, J. M., Friel, T., Jiang, G. C. T., Vrana, K., Sharov, V., Barrón, L., Schöneich, C., Quijano, C., Alvarez, B., et al. (2001) Nitration and Inactivation of Tyrosine Hydroxylase by Peroxynitrite. *J. Biol. Chem. 276* (49), 46017−46023.
(33) Kobayashi, M., Yasukawa, H., Arikawa, T., Deguchi, Y., Mizushima, N., Sakurai, M., Onishi, S., Tagawa, R., Sudo, Y., Okita, N., et al. (2021) Trehalose Induces SQSTM1/P62 Expression and Enhances Lysosomal Activity and Antioxidative Capacity in Adipocytes. *FEBS Open Bio 11* (1), 185−194.
(34) Bardag-Gorce, F., Francis, T., Nan, L., Li, J., Lue, Y. H., French, B. A., and French, S. W. (2005) Modifications in P62 Occur Due to Proteasome Inhibition in Alcoholic Liver Disease. *Life Sci. 77* (20), 2594−2602.
(35) Li, C., Wang, X., Li, X., Qiu, K., Jiao, F., Liu, Y., Kong, Q., Liu, Y., and Wu, Y. (2019) Proteasome Inhibition Activates Autophagy-Lysosome Pathway Associated with TFEB Dephosphorylation and Nuclear Translocation. *Front. Cell Dev. Biol. 7*, 170.
(36) Abokyi, S., Shan, S. w., To, C.-h., Chan, H. H.-l., and Tse, D. Y.-y. (2020) Autophagy Upregulation by the TFEB Inducer Trehalose Protects against Oxidative Damage and Cell Death Associated with NRF2 Inhibition in Human RPE Cells. *Oxid. Med. Cell. Longevity 2020*, 5296341.
(37) Kabeya, Y., Mizushima, N., Ueno, T., Yamamoto, A., Kirisako, T., Noda, T., Kominami, E., Ohsumi, Y., and Yoshimori, T. (2000) LC3, a Mammalian Homologue of Yeast Apg8p, Is Localized in Autophagosome Membranes after Processing. *EMBO J. 19* (21), 5720−5728.
(38) Sarkar, S., Davies, J. E., Huang, Z., Tunnacliffe, A., and Rubinsztein, D. C. (2007) Trehalose, a Novel MTOR-Independent Autophagy Enhancer, Accelerates the Clearance of Mutant Huntingtin and α -Synuclein. *J. Biol. Chem. 282* (8), 5641−5652.
(39) Zhang, J., Yi, M., Zha, L., Chen, S., Li, Z., Li, C., Gong, M., Deng, H., Chu, X., Chen, J., et al. (2016) Sodium Butyrate Induces Endoplasmic Reticulum Stress and Autophagy in Colorectal Cells: Implications for Apoptosis. *PLoS One 11* (1), e0147218.
(40) DeBosch, B. J., Heitmeier, M. R., Mayer, A. L., Higgins, C. B., Crowley, J. R., Kraft, T. E., Chi, M., Newberry, E. P., Chen, Z., Finck, B. N., et al. (2016) Trehalose Inhibits Solute Carrier 2A (SLC2A) Proteins to Induce Autophagy and Prevent Hepatic Steatosis. *Sci. Signaling 9* (416), ra21−ra21.
(41) Minutoli, L., Altavilla, D., Bitto, A., Polito, F., Bellocco, E., Laganà, G., Fiumara, T., Magazù, S., Migliardo, F., Venuti, F. S., et al. (2008) Trehalose: A Biophysics Approach to Modulate the Inflammatory Response during Endotoxic Shock. *Eur. J. Pharmacol. 589* (1−3), 272−280.
(42) Pagliassotti, M. J., Estrada, A. L., Hudson, W. M., Wei, Y., Wang, D., Seals, D. R., Zigler, M. L., and LaRocca, T. J. (2017) Trehalose Supplementation Reduces Hepatic Endoplasmic Reticulum Stress and Inflammatory Signaling in Old Mice. *J. Nutr. Biochem. 45*, 15−23.
(43) Aoki, N., Furukawa, S., Sato, K., Kurokawa, Y., Kanda, S., Takahashi, Y., Mitsuzumi, H., and Itabashi, H. (2010) Supplementation of the Diet of Dairy Cows with Trehalose Results in Milk with Low Lipid Peroxide and High Antioxidant Content. *J. Dairy Sci. 93* (9), 4189−4195.
(44) Aoki, N., Sato, K., Kanda, S., Mukai, K., Obara, Y., and Itabashi, H. (2013) Time Course of Changes in Antioxidant Activity of Milk from Dairy Cows Fed a Trehalose-Supplemented Diet. *Anim. Sci. J. 84* (1), 42−47.
(45) Chen, G., Ran, X., Li, B., Li, Y., He, D., Huang, B., Fu, S., Liu, J., and Wang, W. (2018) Sodium Butyrate Inhibits Inflammation and Maintains Epithelium Barrier Integrity in a TNBS-Induced Inflammatory Bowel Disease Mice Model. *EBioMedicine 30*, 317−325.
(46) Qiao, C.-M., Sun, M.-F., Jia, X.-B., Li, Y., Zhang, B.-P., Zhao, L.-P., Shi, Y., Zhou, Z.-L., Zhu, Y.-L., Cui, C., et al. (2020) Sodium Butyrate Exacerbates Parkinson's Disease by Aggravating Neuroinflammation and Colonic Inflammation in MPTP-Induced Mice Model. *Neurochem. Res. 45* (9), 2128−2142.
(47) Sampson, T. R., Debelius, J. W., Thron, T., Janssen, S., Shastri, G. G., Ilhan, Z. E., Challis, C., Schretter, C. E., Rocha, S., Gradinaru, V., et al. (2016) Gut Microbiota Regulate Motor Deficits and Neuroinflammation in a Model of Parkinson's Disease. *Cell 167* (6), 1469−1480.
(48) Tanaka, M., Machida, Y., Niu, S., Ikeda, T., Jana, N. R., Doi, H., Kurosawa, M., Nekooki, M., and Nukina, N. (2004) Trehalose Alleviates Polyglutamine-Mediated Pathology in a Mouse Model of Huntington Disease. *Nat. Med. 10* (2), 148−154.
(49) Castillo, K., Nassif, M., Valenzuela, V., Rojas, F., Matus, S., Mercado, G., Court, F. A., van Zundert, B., and Hetz, C. (2013) Trehalose Delays the Progression of Amyotrophic Lateral Sclerosis by Enhancing Autophagy in Motoneurons. *Autophagy 9* (9), 1308−1320.
(50) Lee, H.-J., Yoon, Y.-S., and Lee, S.-J. (2018) Mechanism of Neuroprotection by Trehalose: Controversy Surrounding Autophagy Induction. *Cell Death Dis. 9*, 712.
(51) Kam, T.-I., Mao, X., Park, H., Chou, S.-C., Karuppagounder, S. S., Umanah, G. E., Yun, S. P., Brahmachari, S., Panicker, N., and Chen, R. (2018) Poly(ADP-Ribose) Drives Pathologic α -Synuclein Neurodegeneration in Parkinson's Disease. *Science (Washington, DC, U. S.) 362* (6414), eaat8407.
(52) Sharma, S., and Deshmukh, R. (2015) Vinpocetine Attenuates MPTP-Induced Motor Deficit and Biochemical Abnormalities in Wistar Rats. *Neuroscience 286*, 393−403.
(53) Crusio, W. E. The Genetics of Exploratory Behavior. (2013) In *Behavioral Genetics of the Mouse* (Crusio, W. E., Sluyter, F., Gerlai, R. T., and Pietropaolo, S., Eds.), pp 148−154, Cambridge University Press, Cambridge, UK.
(54) Crusio, W. E., Sluyter, F., and Gerlai, R. T. Ethogram of the Mouse. (2013) In *Behavioral Genetics of the Mouse* (Crusio, W. E., Sluyter, F., Gerlai, R. T., and Pietropaolo, S., Eds.), pp 17−22, Cambridge University Press: Cambridge, UK.
(55) Luong, T. N., Carlisle, H. J., Southwell, A., and Patterson, P. H. (2011) Assessment of Motor Balance and Coordination in Mice Using the Balance Beam. *J. Visualized Exp.* No. 49, e2376.
(56) Quillfeldt, J. A. Behavioral Methods to Study Learning and Memory in Rats. (2016) In *Rodent Model as Tools in Ethical Biomedical Research*, pp 271−311, Springer, Cham.
(57) Antunes, M., and Biala, G. (2012) The Novel Object Recognition Memory: Neurobiology, Test Procedure, and Its Modifications. *Cogn. Process. 13* (2), 93−110.
(58) Lowry, O. H., Rosebrough, N. J., Farr, A. L., Randall, R. J., et al. (1951) Protein Measurement with the Folin Phenol Reagent. *J. Biol. Chem. 193*, 265−275.
(59) K C, S., Kakoty, V., Marathe, S., Chitkara, D., and Taliyan, R. (2021) Exploring the Neuroprotective Potential of Rosiglitazone Embedded Nanocarrier System on Streptozotocin Induced Mice Model of Alzheimer's Disease. *Neurotoxic. Res. 39*, 240−255.

https://doi.org/10.1021/acschemneuro.1c00144
ACS Chem. Neurosci. 2021, 12, 2643−2660